Metastable dark energy models in light of *Planck* 2018 data: Alleviating the H_0 tension

Weiqiang Yang,[1,*] Eleonora Di Valentino,[2,†] Supriya Pan,[3,‡] Spyros Basilakos,[4,5,§] and Andronikos Paliathanasis[6,7,∥]

[1]*Department of Physics, Liaoning Normal University, Dalian 116029, People's Republic of China*
[2]*Jodrell Bank Center for Astrophysics, School of Physics and Astronomy, University of Manchester, Oxford Road, Manchester M13 9PL, United Kingdom*
[3]*Department of Mathematics, Presidency University, 86/1 College Street, Kolkata 700073, India*
[4]*Academy of Athens, Research Center for Astronomy and Applied Mathematics, Soranou Efessiou 4, 115 27 Athens, Greece*
[5]*National Observatory of Athens, Lofos Nymfon, 11852 Athens, Greece*
[6]*Institute of Systems Science, Durban University of Technology, PO Box 1334, Durban 4000, Republic of South Africa*
[7]*Instituto de Ciencias Físicas y Matemáticas, Universidad Austral de Chile, Valdivia 5090000, Chile*

(Received 15 January 2020; accepted 12 August 2020; published 3 September 2020)

We investigate the recently introduced metastable dark energy (DE) models after the final *Planck* 2018 legacy release. The essence of the present work is to analyze their evolution at the level of perturbations. Our analyses show that both the metastable dark energy models considered in this article, are excellent candidates to alleviate the H_0 tension. In particular, for the present models, *Planck* 2018 alone can alleviate the H_0 tension within 68% CL. Along with the final cosmic microwave background data from the *Planck* 2018 legacy release, we also include external cosmological datasets in order to asses the robustness of our findings.

DOI: 10.1103/PhysRevD.102.063503

I. INTRODUCTION

The nature of dark energy (DE) or geometrical dark energy (GDE) is one of the intrinsic queries of modern cosmology that we are still looking for. According to the analyses of the high quality observational data, the present accelerating phase of the universe is quite well described in the framework of the general relativity together with a cosmological constant—the so called ΛCDM model. However, due to many theoretical and observational shortcomings associated with the ΛCDM cosmology, searches for alternative descriptions have been necessary. Apart from the well-known cosmological constant/fine tuning and cosmic coincidence problems affecting the ΛCDM scenario, recent observations indicate that the CMB measurements of some key cosmological parameters within this minimal ΛCDM scenario do not match with the values measured by other cosmological probes. Specifically, one is the long standing H_0 tension (above 4σ) between the estimated value of H_0 provided by *Planck* [1] (in agreement with [2–24]) and that one measured by the SH0ES collaboration [25] (see also [26–41]). Despite the above measurements, there are local expansion estimates which indicates that the tension is close to $\sim 2\sigma$, i.e., preferring a lower value with respect to the SH0ES result. Moreover, in Ref. [42] it has been speculated that a systematic bias of 0.1–0.15 *mag* in the intercept of the Cepheid period-luminosity relations of SH0ES galaxies could resolve the H_0 tension. However, the final result from the Maser Cosmology Project [43], completely independent from these considerations, measuring geometric distances to 6 masers in the Hubble flow, found $H_0 = (73.9 \pm 3.0)$ km/s/Mpc, completely in agreement with the SH0ES value. The other one is the S_8 tension between *Planck* and the cosmic shear measurements KiDS-450 [44–46], Dark Energy Survey (DES) [47,48] or CFHTLenS [49–51]. Furthermore, when a curvature is considered into the cosmic picture [52], all these tensions are exacerbated revealing a possible crisis for the cosmology. Thus, in order to circumvent these problems, several alternative cosmological models have been introduced in the literature aiming to solve or alleviate such tensions in an effective way. In the literature there is a large family of models that alleviate the H_0 tension among which "multiparameter" dark energy [53–57], early dark energy [58–63], interacting dark energy [64–73], modified gravity models [74–76], and the list goes on (see [13,16,31,77–110]. On the other hand,

*d11102004@163.com
†eleonora.divalentino@manchester.ac.uk
‡supriya.maths@presiuniv.ac.in
§svasil@academyofathens.gr
∥anpaliat@phys.uoa.gr

for the well known $S_8 = \sigma_8 \sqrt{\Omega_{m0}/0.3}$ tension we refer the reader the following works [56,71,99,111–114]. The above family of models provide a framework of alleviating such tensions within 3σ, but the problem still remains open.

In this article we consider two metastable DE models introduced recently by Shafieloo *et al.* [94] (also see [95]). The basic ingredient of these models is that the decay of DE does not depend on the external parameters, such as the expansion rate of the universe etc. These models depend only on the intrinsic properties of DE. Thus, it is expected that metastable DE models could explore some inherent nature of the dark sector, specially the DE. Our observational constraints on the metastable DE models should be considered stringent for the following reasons: (i) we have considered the cosmological perturbations for the models, an indispensable tool to understand the large scale structure of the universe, and (ii) we have included the final *Planck* 2018 data [1,115,116]. A quick observation from our analyses is that the metastable DE models are able to alleviate the H_0 tension.

The article is organized in the following way. In Sec. II, assuming the Friedmann-Lemaître-Robertson-Walker (FLRW) universe, we present the gravitational equations and two metastable DE models that we wish to study in this work. In Sec. III we discuss the observational data and the methodology applied to constrain the models. Then we discuss the results of our analyses in Sec. IV. Finally, in Sec. V we close our work with a brief summary of all the findings.

II. METASTABLE DARK ENERGY MODELS

In this section we review two metastable DE models introduced recently by [94,95]. We assume the spatially flat Friedmann-Lemaître-Robertson-Walker (FLRW) geometry which is characterized by the line element $ds^2 = -dt^2 + a^2(t)[dx^2 + dy^2 + dz^2]$, where $a(t)$ (hereafter a) is the scale factor of the universe. The gravitational sector of the universe follows Einstein's general relativity where in addition we assume that the matter content of the universe is minimally coupled to gravity. Further, we assume that the entire universe is comprised of baryons, radiation, pressureless dark matter and a dark energy fluid. Throughout the present work we shall identify ρ_i and p_i as the energy density and pressure of the ith fluid. Here, $i = \{b, r, c, x\}$ stands for baryons (b), radiation (r), pressureless or cold dark matter (c) and DE (x). Within this framework, one could write down the Einstein's field equations:

$$3H^2 = \frac{8\pi G}{3}\sum_i \rho_i, \tag{1}$$

$$2\dot{H} + 3H^2 = -4\pi G \sum_i p_i, \tag{2}$$

where an overhead dot denotes the derivative with respect to the cosmic time; $H \equiv \dot{a}/a$ is the Hubble rate of the FLRW universe and $8\pi G$ is the Einstein's gravitational constant (G is the Newton's gravitational constant). Let us note that using either the Bianchi's identity or using the gravitational equations (1) and (2), one could derive the conservation equation of the total fluid

$$\sum_i \dot{\rho}_i + 3H\sum_i(\rho_i + p_i) = 0. \tag{3}$$

So, out of the three equations, namely, Eqs. (1)–(3), only two of them are independent. Since DE plays a crucial role in the dynamics of the universe, over the last two decades, several forms of DE have been studied in the literature. In most of the cases, it has been assumed that DE density depends on the external parameters, such as the scale factor, a, of the FLRW universe; its expansion rate, H; or its scalar curvature. While one may naturally consider a scenario in which DE depends from its intrinsic composition and structure. The motivation of the metastable DE models is along the latter lines. In the following we shall introduce two metastable DE models and discuss their physical origin.

A. Model I

The first metastable DE model that we aim to study follows the evolution law [94,95]:

$$\dot{\rho}_x = -\Gamma \rho_x, \tag{4}$$

where ρ_x, as already mentioned, denotes the energy density of DE and Γ is a constant which could be either positive or negative and its dimension is same as that of the Hubble rate, H, of the FLRW universe. Note that, $\Gamma = 0$ implies $\rho_x =$ constant, featuring the cosmological constant. Note further that other cosmic fluids, namely baryons, radiation and cold dark matter follow the usual conservation equation, that means, $\dot{\rho}_i + 3H(p_i + \rho_i) = 0$, where $i = \{b, r, c\}$. The evolution of DE characterized in Eq. (4) is exponential, and for $\Gamma > 0$ DE density has a decaying character, while for $\Gamma < 0$ DE density is increasing. This kind of evolution is actually motivated from the "radioactive decay" scheme in which unstable nuclei and elementary particles may decay. Moreover, as we have already mentioned, the energy densities of radiation, baryons, and cold dark matter obey the standard scaling laws implying that this model can be viewed in the context of dynamical dark energy. Hence, one can introduce a homogeneous scalar field ϕ [117,118] rolling down the potential energy $V(\phi)$, and therefore it could resemble a scalar field model of DE. Now, if we focus on the evolution of DE as given in Eq. (4), that means, $\dot{\rho}_x + \Gamma\rho_x = 0$, one could quickly find its equivalent structure by comparing it with the standard evolution of DE

$$\dot{\rho}_x + 3H(1 + w_x)\rho_x = 0, \tag{5}$$

which naturally introduces a dynamical equation of state of DE, $w_x = p_x/\rho_x$. Thus, comparing (4) and (5), one could determine, $w_x = -1 + \frac{\Gamma/H_0}{3H/H_0}$, where we introduce H_0, i.e., the present value of H. In other words, Γ will give us an estimate of the deviation of the dark energy equation of state from the cosmological constant.

Let us now proceed with the evolution of this model at the level of perturbations. Here we consider the perturbed FLRW metric in the synchronous gauge [119]

$$ds^2 = a^2(\tau)[-d\tau^2 + (\delta_{ij} + h_{ij})dx^i dx^j], \tag{6}$$

where τ is the conformal time; δ_{ij}, h_{ij} respectively denote the unperturbed and perturbed metric tensors. Now, for the above metric (6), using the conservation equation for the total fluid, one can conveniently derive the corresponding evolution equations Fourier space k, and they are

$$\delta'_x = -(1+w_x)\left(\theta_x + \frac{h'}{2}\right) - 3\mathcal{H}(c_{sx}^2 - w_x) \times \left[\delta_x + 3\mathcal{H}(1+w_x)\frac{\theta_x}{k^2}\right] - 3\mathcal{H}w'_x\frac{\theta_x}{k^2}, \tag{7}$$

$$\theta'_x = -\mathcal{H}(1-3c_{sx}^2)\theta_x + \frac{c_{sx}^2}{1+w_x}k^2\delta_x, \tag{8}$$

$$\delta'_c = -\left(\theta_c + \frac{h'}{2}\right), \tag{9}$$

$$\theta'_c = -\mathcal{H}\theta_c, \tag{10}$$

where the primes attached to any quantity denote the derivative of that quantity with respect to the conformal time τ; $\mathcal{H} = a'/a$, denotes the conformal Hubble factor; $h = h^j_j$ is the trace of the metric perturbations h_{ij}; $\theta_i \equiv i\kappa^j v_j$ (here $i = c, x$) is the divergence of the ith fluid velocity. Finally, $\delta_i = \delta\rho_i/\rho_i$ denotes the density perturbation for the ith fluid, that means δ_x is the density perturbation for the dark energy fluid while δ_c refers to the density perturbation for the cold dark matter fluid. Notice that $c_{sx}^2 = \delta p_x/\delta\rho_x$, is the effective sound speed of the DE perturbations in the rest frame [120] (the corresponding quantity for matter is zero in the dust case), which determines the amount of DE clustering and it can be treated as a free parameter without any problem. However, we need to have in mind that the inclusion of the sound speed as a free parameter actually increases the degeneracy among the model parameters. On the other hand, for barotropic DE with constant equation of state w_x, $c_{sx}^2 = w_x < 0$, and hence instabilities appear in the DE fluid [121,122]. In order to avoid instabilities one has to impose $c_{sx}^2 > 0$ [121,122]. It is well known that in the case of a homogeneous dark energy we have $c_{sx}^2 = 1$, hence, the corresponding pressure suppresses any DE fluctuations at subhorizon scales, and consequently, the quantities δ_x and θ_x are vanished. On the other hand, for $c_{sx}^2 = 0$, DE clusters similar to that of dark matter perturbations. The clustering of DE modifies the evolution of dark matter fluctuations perturbations (for more discussion see [123–128] and the references therein). In the current paper we have set $c_{sx}^2 = 1$, which implies that dark energy is nonclustering, hence one should consider the perturbation equations along with the background ones.

In this context, let us now provide the temperature anisotropies of the CMB spectra and the matter power spectra of Model I. In Fig. 1, we have shown the corresponding plots for various numerical values of the dimensionless parameter Γ/H_0. In particular, we show the CMB TT spectra in the left panel and matter power spectra in the right one. One can clearly see that even if we increase the magnitude of Γ/H_0, there is no significant changes in the spectra. However, a mild deviation from

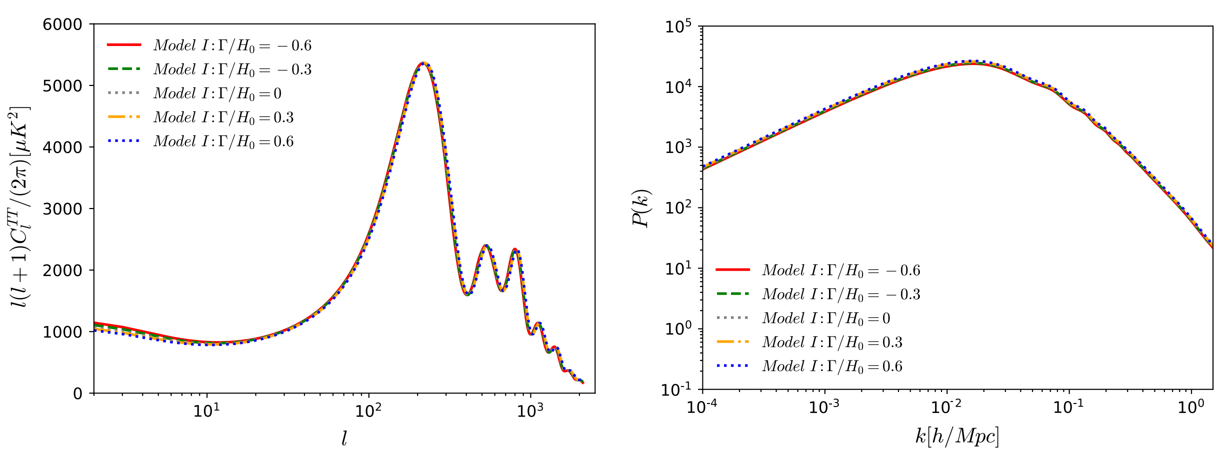

FIG. 1. CMB temperature angular power spectra (upper left) and matter power spectra (upper right) for different values of the dimensionless parameter Γ/H_0 of Model I have been shown.

ΛCDM ($\Gamma/H_0 = 0$) appears only for low multipoles of the CMB spectra.

B. Model II

We now introduce the second metastable DE model in this work which is an interacting dark scenario between a pressureless dark matter and vacuum energy characterized by the conservation equations:

$$\dot{\rho}_x = -Q, \tag{11}$$

$$\dot{\rho}_c + 3H\rho_c = Q, \tag{12}$$

where Q refers to an interaction function between these dark sectors. Now, given a specific functional form for Q, one may determine the dynamics of the interacting universe by solving the above conservation equations together with the Hubble equation in Eq. (1). The possibility of an interaction in the cosmic sector was initially motivated to explain the cosmological constant problem [129] and later this theory was found to provide with an appealing explanation to the cosmic coincidence problem [130–133]. These results motivated several investigators to work in this region. Therefore, in the last two decades, cosmological scenarios that allow interaction between the cosmic fluids, namely between the dark sectors of the universe have been extensively studied, see for instance [121,122,134–177]. For these models it has been proposed that interaction function takes the following forms $Q \propto \rho_c$, $Q \propto \rho_x$, $Q \propto (\rho_c + \rho_x)$, while there are also some other choices which include more complex forms as far as Q is concerned (see [122]).

We would like to stress our original approach regarding the present metastable model has been phenomenological. Phenomenology is a valid and frequently used method in theoretical cosmology, especially over the last decade. Indeed a plethora of papers have been published in metastable dark energy studies, without necessarily providing a physical interpretation. Nevertheless, since Model II allows interactions in the dark sector we would like to point out that there are several attempts regarding the physical interpretation of these interactions based on action principles [178–183]. We remind the reader that in this case cold DM interacts with DE (or vacuum), hence the cold DM density does not follow the standard power-law a^{-3}.

Specifically, it has been found in Ref. [183] that the interaction function $Q \propto \rho_x$ has a field theoretic description. Moreover, following the recent works [184,185] if we treat ρ_x as a running vacuum density $\rho_\Lambda(t)$ then Model II can be seen within the context of a string-inspired effective theory in the presence of a Kalb-Ramond (KR) gravitational axion field which descends from the antisymmetric tensor of the massless gravitational string multiplet.

In the present article, we shall use $Q = \Gamma\rho_x$ as considered in [94,95] where Γ is the coupling parameter. Here we assume that Γ is constant and it has the same dimension as that of the Hubble constant, hence Γ/H_0 is the dimensionless quantity which we attempt to place constraints from the observational data. Notice that the present interaction rate does not depend on any parameter related to the expansion of the universe, for instance the Hubble rate of the FLRW universe as considered in many works just for mathematical convenience, and this is the basic feature of the metastable DE models. The sign of Γ determines the flow of energy between the dark two sectors. For $\Gamma > 0$, DE decays into DM while for $\Gamma < 0$, the situation is reversed, that means energy flows from DM to DE. We consider a general picture allowing Γ to take both positive and negative values, with $\Gamma = 0$ recovering the noninteracting ΛCDM cosmology. Having presented the gravitational equations for this model at the level of background, one can now proceed toward its understanding at the level of perturbations.

In order to understand the evolution of the model at the level of perturbations, we recall the perturbed FLRW metric in the synchronous gauge given in Eq. (6). Within this formalism, one can write down the perturbations equations of the above model as [186,187]:

$$\delta_c' = -\left(\theta_c + \frac{h'}{2}\right) - \frac{aQ}{\rho_c}\delta_c = -\frac{h'}{2} - \left(\frac{a\Gamma\rho_x}{\rho_c}\right)\delta_c, \tag{13}$$

$$\theta_c' = -\mathcal{H}\theta_c, \tag{14}$$

where prime denotes the differentiation with respect to the conformal time; h is the trace of the metric perturbations h_{ij} [see the perturbed metric (6)]; and δ_c is the density perturbations for the CDM fluid and θ_c is the volume expansion scalar for the CDM fluid. Notice here that, following [186], we consider an energy flow parallel to the four velocity of the CDM fluid. As a result, CDM particles follow geodesics as in ΛCDM and consequently, the vacuum energy perturbations will vanish in the CDM-comoving frame. Now, from the residual gauge freedom in the synchronous gauge, one may take $\theta_c = 0$ as we have taken, and hence $\theta_c' = 0$.

We now proceed toward the understanding of the effects of this model through various quantities. In Fig. 2 we plot the temperature anisotropy of the CMB spectra and the matter power spectra for various numerical values of the dimensionless parameter Γ/H_0. Specifically, the left panel of Fig. 2 shows the CMB TT power spectra and the right panel of Fig. 2 shows the matter power spectra. The features of the spectra are quite different compared to the Model I. As one can see from the CMB TT power spectra, a mild change in the dimensionless coupling parameter Γ/H_0 produces an observable change in the spectrum and this clearly distinguishes Model II from Model I (see Fig. 1). In fact, for negative values of Γ/H_0 (DM decaying into DE), the amplitude of the first acoustic peak in the CMB TT spectra decreases. The opposite scenario holds when the energy flow takes place

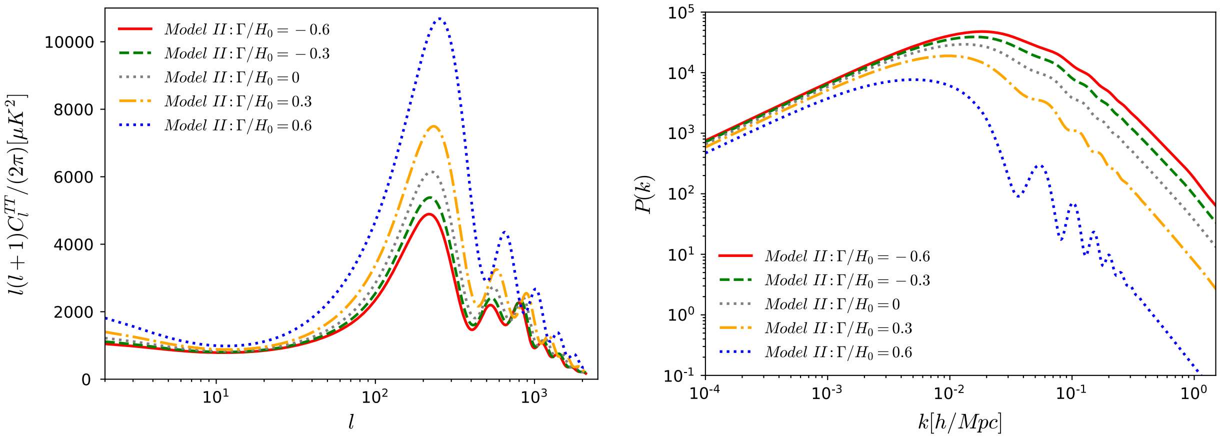

FIG. 2. CMB temperature angular power spectra (upper left) and matter power spectra (upper right) for different values of the dimensionless coupling parameter Γ/H_0 of Model II have been shown.

from DE to DM ($\Gamma > 0$). Similar effects are observed in the matter power spectra, but in this case when Γ/H_0 increases, the amplitude of the matter power spectrum becomes more suppressed.

III. OBSERVATIONAL DATA AND METHODOLOGY

This section is devoted to describe the observational datasets, statistical techniques and the priors imposed on various free parameters related to the aforementioned metastable dark energy models, namely, Model I and Model II.

Our baseline dataset is *Planck* 2018, i.e., the latest cosmic microwave background (CMB) temperature and polarization angular power spectra $plikTTTEEE + lowl + lowE$ from the final 2018 *Planck* legacy release [1,115,116]. Moreover, we test the robustness of our result by including a few cosmological probes, choosing a subset between all the datasets available in the literature (see for example [188]):

(i) BAO: Measurements of the BAO data from different astronomical missions [189–191] have been used.

(ii) DES: The galaxy clustering and cosmic shear measurements from the Dark Energy Survey (DES) combined-probe Year 1 results [47,48,192], as adopted by the Planck collaboration in [1] have been analyzed.

(iii) R19: The recent measurement of the Hubble constant from a reanalysis of the Hubble Space Telescope data using Cepheids as calibrators, giving $H_0 = 74.03 \pm 1.42$ km/s/Mpc at 68% CL [25] has been considered. It is important to comment that this H_0 value is in tension at 4.4σ with the Planck's estimation within the ΛCDM cosmological set-up.

To constrain the metastable DE scenarios we use our modified version of the publicly available markov chain monte carlo package CosmoMC [193,194], an excellent cosmological code having a fine convergence diagnostic by Gelman-Rubin [195]. This code includes the support for *Planck* 2018 likelihood [115,116]. The models we are considering have one extra free parameter, Γ, compared to the flat ΛCDM model (six-parameters). Let us also mention that in the current analysis, we have fixed the sound speed of DE to unity ($c_{sx}^2 = 1$), which means that we are dealing with a homogeneous DE. Therefore, the parameter space of the models is

$$\mathcal{P}_1 \equiv \{\Omega_b h^2, \Omega_c h^2, 100\theta_{MC}, \tau, n_s, \log[10^{10} A_s], \Gamma/H_0\}, \tag{15}$$

where $\Omega_b h^2$, $\Omega_c h^2$, are the dimensionless densities of baryons and cold dark matter, respectively; θ_{MC} denotes the ratio of the sound horizon to the angular diameter distance; τ refers to the reionization optical depth; n_s denotes the scalar spectral index; A_s being the amplitude of the primordial scalar power spectrum; and Γ/H_0 being the free parameter of the metastable models normalized to the Hubble constant value. For the statistical analyses, we have imposed flat priors (see Table I) on the above free parameters.

IV. RESULTS AND ANALYSES

In this section we present the observational constraints on the present metastable DE scenarios by considering data from *Planck* 2018 and other cosmological probes III. Regarding the initial conditions that are used during the analysis the situation is as follows. For the first model of our consideration, namely Model I, by following the notations of [196], we have assumed adiabatic initial conditions. Now, although Model II represents a coupled cosmic scenario, if one assumes adiabatic initial conditions for the standard components, namely radiation and baryons, then the interacting dark fluids also follow the adiabatic initial conditions, see [143,146,197]. The observational constraints for both the

TABLE I. We show the flat priors on the free parameters of both metastable DE models for the statistical simulations.

Parameter	Prior (Model I)	Prior (Model II)
$\Omega_b h^2$	[0.005, 0.1]	[0.005, 0.1]
$\Omega_c h^2$	[0.01, 0.99]	[0.01, 0.99]
τ	[0.01, 0.8]	[0.01, 0.8]
n_s	[0.5, 1.5]	[0.5, 1.5]
$\log[10^{10}A_s]$	[2.4, 4]	[2.4, 4]
$100\theta_{MC}$	[0.5, 10]	[0.5, 10]
Γ/H_0	$[-1, 1]$	$[-1, 0.7]$

models are summarized in Tables II (for Model 1) and Table IV (for Model 2). Further, the constraints on the ΛCDM cosmology (equivalently, $\Gamma = 0$) have been shown in Table III for comparing the models with $\Gamma \neq 0$. Additionally, in Figs. 3 and 6 we present the corresponding contour plots (68% and 95% CL) for each model respectively.

A. Model I

Let us start with the presentation of the results for Model I. Using the data from *Planck* 2018 only (see second column of Table II) we observe that the dimensionless parameter Γ/H_0 deviates from zero at more than 1σ, and it is completely unconstrained at 95% CL. We find that this parameter is correlated with most of the key parameters of the model. The fact that the Γ/H_0 is unconstrained from *Planck* 2018 data, can be easily verified if we look at Fig. 1. We notice a strong positive correlation of the Hubble constant, H_0, with Γ/H_0, hence H_0 takes a relatively large value with very high error bars ($H_0 = 69.3^{+5.9}_{-3.5}$, 68% C.L., *Planck* 2018) with respect to that of ΛCDM model (see Table III). Therefore, in the context of Model I the H_0 measurement provided by *Planck* 2018 is compatible (within one standard deviation) with that of R19. Thanks to the geometrical degeneracy between H_0 and Ω_{m0} appeared in the CMB data, we also find that Model I prefers a lower value of the matter density. Indeed as we can see from Fig. 4, there is a strong anticorrelation between Γ/H_0 and Ω_{m0}.

Combining BAOs and *Planck* 2018 data we can place constraints on Γ/H_0 at 95% C.L., (see third column of II and the 3D scattered plot of Fig. 4). This is due to the strong power of BAO data in constraining Ω_{m0} which anticorrelates with Γ/H_0. Notice, that in this case we have $\Gamma/H_0 = 0$, i.e., in agreement with the ΛCDM model, within 1σ. Further, regarding H_0 using *Planck* 2018 + BAO dataset, we observe 2.6σ compatibility ($H_0 = 68.3^{+1.6}_{-1.7}$) with the corresponding value obtained R19, while in the case of the concordance ΛCDM model the difference is close to $\sim 4.4\sigma$.

Now let us test the combination *Planck* 2018 + DES data. The results of *Planck* 2018 + DES combination are summarized in the fourth column of Table II. In this case we have a lower limit of Γ/H_0, which is above zero (i.e., a cosmological constant model), at 2σ level, implying a decaying DE component. Concerning Ω_{m0}, its best fit value becomes relatively low, namely $\Omega_{m0} = 0.263^{+0.012}_{-0.027}$ (68% C.L., *Planck* 2018 + DES). Thanks to the three-parameter correlation shown in Fig. 4, we find that the best value of H_0 tends to that of R19 together, while the corresponding errors bars are quite large.

Now the statistical results of the combined dataset *Planck* 2018 + R19 are shown in the fifth column of Table II. For this combination of data we find a strong indication of decaying DE with $\Gamma/H_0 > 0$ at more than 2σ, namely we obtain $\Gamma/H_0 > 0.53$ at 95% C.L. These constraints are in very good agreement with those of *Planck* 2018 + DES, showing a resolution of the tension with the cosmic shear data at the same time.

Finally, using *Planck* 2018 + BAO + DES + R19 we present the corresponding results in the last column of

TABLE II. Summary of the observational constraints and lower limits at 68% and 95% CL on the cosmological scenario driven by the metastable DE scenario, *Model I*, using different observational datasets. The parameters are varying in the ranges described in Table I.

Parameters	*Planck* 2018	*Planck* 2018 + BAO	*Planck* 2018 + DES	*Planck* 2018 + R19	*Planck* 2018 + BAO + DES + R19
$\Omega_c h^2$	$0.1205^{+0.0014+0.0027}_{-0.0014-0.0027}$	$0.1197^{+0.0013+0.0024}_{-0.0012-0.0024}$	$0.1183^{+0.0011+0.0022}_{-0.0011-0.0022}$	$0.1203^{+0.0013+0.0026}_{-0.0013-0.0025}$	$0.1190^{+0.00098+0.0019}_{-0.00099-0.0020}$
$\Omega_b h^2$	$0.02231^{+0.00015+0.00029}_{-0.00015-0.00031}$	$0.02236^{+0.00015+0.00028}_{-0.00014-0.00029}$	$0.02246^{+0.00014+0.00028}_{-0.00014-0.00028}$	$0.02232^{+0.00014+0.00029}_{-0.00016-0.00029}$	$0.02243^{+0.00014+0.00026}_{-0.00014-0.00026}$
$100\theta_{MC}$	$1.04062^{+0.00031+0.00060}_{-0.00030-0.00062}$	$1.04072^{+0.00029+0.00061}_{-0.00031-0.00060}$	$1.04084^{+0.00030+0.00061}_{-0.00032-0.00060}$	$1.04065^{+0.00031+0.00064}_{-0.00032-0.00061}$	$1.04077^{+0.00031+0.00058}_{-0.00030-0.00058}$
τ	$0.054^{+0.0074+0.015}_{-0.0074-0.015}$	$0.056^{+0.0077+0.017}_{-0.0079-0.016}$	$0.055^{+0.0077+0.017}_{-0.0077-0.016}$	$0.055^{+0.0077+0.016}_{-0.0084-0.015}$	$0.053^{+0.0073+0.015}_{-0.0073-0.015}$
n_s	$0.9722^{+0.0043+0.0086}_{-0.0044-0.0086}$	$0.9740^{+0.0040+0.0078}_{-0.0040-0.0078}$	$0.9766^{+0.0039+0.0078}_{-0.0040-0.0077}$	$0.9729^{+0.0043+0.0083}_{-0.0042-0.0084}$	$0.9750^{+0.0038+0.0074}_{-0.0038-0.0072}$
$\ln(10^{10}A_s)$	$3.055^{+0.015+0.031}_{-0.015-0.031}$	$3.056^{+0.016+0.035}_{-0.017-0.033}$	$3.051^{+0.016+0.033}_{-0.016-0.031}$	$3.055^{+0.016+0.032}_{-0.017-0.031}$	$3.048^{+0.015+0.032}_{-0.016-0.029}$
Γ/H_0	> 0.04, unconstrained	$0.17^{+0.26+0.47}_{-0.23-0.47}$	$> 0.54 > -0.01$	$0.78^{+0.19}_{-0.08} > 0.53$	$> 0.367 > 0.193$
Ω_{m0}	$0.303^{+0.026+0.080}_{-0.053-0.065}$	$0.306^{+0.014+0.028}_{-0.016-0.026}$	$0.263^{+0.012+0.048}_{-0.027-0.037}$	$0.263^{+0.0089+0.020}_{-0.011-0.019}$	$0.275^{+0.0076+0.018}_{-0.0089-0.017}$
H_0	$69.3^{+5.9+7.3}_{-3.5-8.3}$	$68.3^{+1.6+3.2}_{-1.7-3.4}$	$73.6^{+3.7+4.9}_{-1.8-6.2}$	$73.8^{+1.4+2.5}_{-1.2-2.6}$	$71.94^{+1.08+2.21}_{-1.08-2.42}$
χ^2	2771.046	2779.456	3293.906	2771.620	3313.11

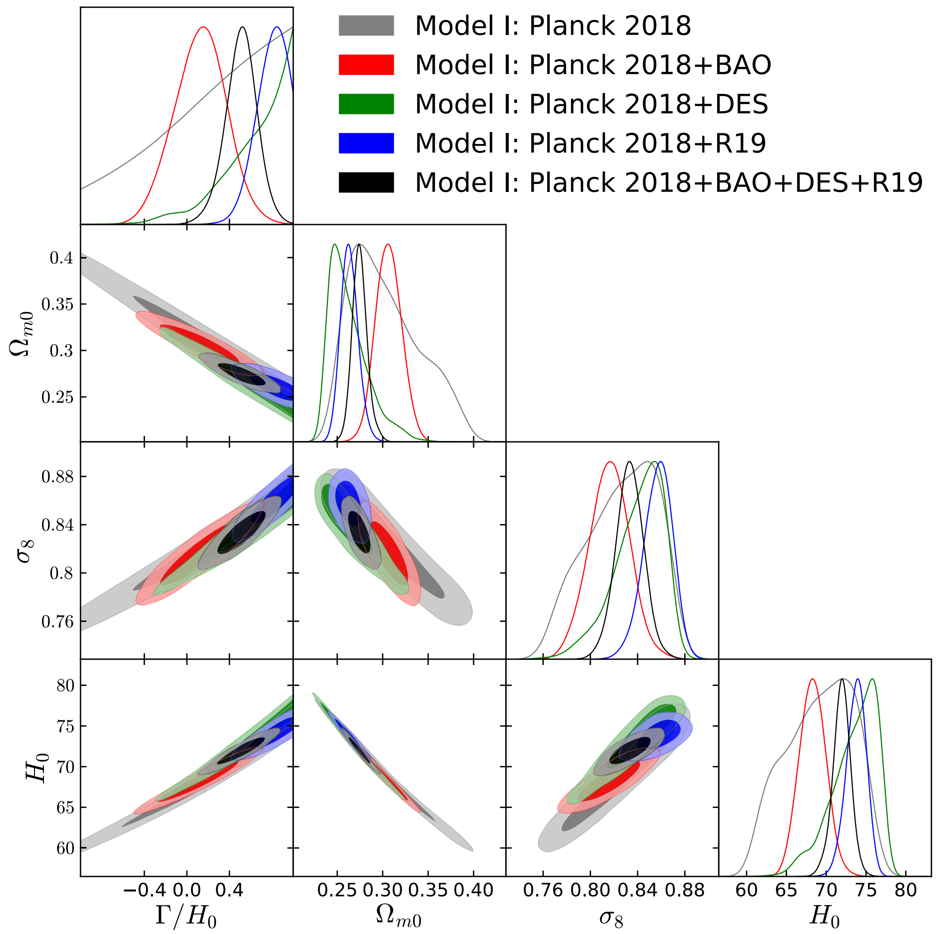

FIG. 3. 68% and 95% CL constraints on the metastable DE scenario, *Model I*, using various observational datasets have been displayed.

Table II. Also in this case Γ/H_0 deviates from zero at 2σ and we observe 1σ compatibility of all acquired parameter values with the corresponding values obtained from *Planck* 2018 + DES data.

Lastly, for a better understanding on the constraints on H_0 of different observational datasets, in Fig. 5 we present all of them in a whisker plot diagram, where we display the constraints on H_0 from the observational datasets employed for this model as well as we show two different vertical bands referring to the constraints from *Planck* 2018 (the vertical grey band) [1] and the local estimation (the vertical sky-blue band) from R19 [25].

TABLE III. We show the constraints on the ΛCDM scenario (corresponding to $\Gamma = 0$) using the same observational data.

Parameters	*Planck* 2018	*Planck* 2018 + BAO	*Planck* 2018 + DES	*Planck* 2018 + R19	*Planck* 2018 + BAO + DES + R19
$\Omega_c h^2$	$0.1202^{+0.0014+0.0027}_{-0.0014-0.0026}$	$0.1193^{+0.0010+0.0019}_{-0.0010-0.0020}$	$0.1179^{+0.0010+0.0021}_{-0.0010-0.0021}$	$0.1179^{+0.0012+0.0025}_{-0.0012-0.0025}$	$0.1172^{+0.00084+0.0017}_{-0.00094-0.0016}$
$\Omega_b h^2$	$0.02236^{+0.00015+0.00029}_{-0.00015-0.00028}$	$0.02243^{+0.00014+0.00027}_{-0.00014-0.00027}$	$0.02251^{+0.00014+0.00027}_{-0.00014-0.00026}$	$0.02255^{+0.00014+0.00028}_{-0.00014-0.00028}$	$0.02260^{+0.00013+0.00025}_{-0.00012-0.00026}$
$100\theta_{MC}$	$1.04091^{+0.00030+0.00061}_{-0.00031-0.00061}$	$1.04100^{+0.00029+0.00057}_{-0.00029-0.00058}$	$1.04113^{+0.00030+0.00060}_{-0.00030-0.00059}$	$1.04120^{+0.00030+0.00057}_{-0.00030-0.00059}$	$1.04125^{+0.00029+0.00055}_{-0.00029-0.00056}$
τ	$0.054^{+0.0071+0.016}_{-0.0083-0.015}$	$0.055^{+0.0076+0.017}_{-0.0084-0.015}$	$0.055^{+0.0072+0.016}_{-0.0081-0.015}$	$0.058^{+0.0075+0.016}_{-0.0085-0.016}$	$0.056^{+0.0071+0.015}_{-0.0073-0.015}$
n_s	$0.9647^{+0.0044+0.0085}_{-0.0043-0.0084}$	$0.9669^{+0.0038+0.0075}_{-0.0038-0.0073}$	$0.9694^{+0.0039+0.0078}_{-0.0039-0.0078}$	$0.9704^{+0.0041+0.0082}_{-0.0041-0.0083}$	$0.9715^{+0.0035+0.0072}_{-0.0036-0.0072}$
$\ln(10^{10}A_s)$	$3.045^{+0.015+0.032}_{-0.017-0.030}$	$3.045^{+0.016+0.034}_{-0.016-0.032}$	$3.039^{+0.015+0.032}_{-0.017-0.030}$	$3.047^{+0.016+0.033}_{-0.017-0.034}$	$3.042^{+0.015+0.030}_{-0.015-0.028}$
Ω_{m0}	$0.317^{+0.0084+0.017}_{-0.0084-0.016}$	$0.311^{+0.0060+0.012}_{-0.0060-0.012}$	$0.303^{+0.0061+0.012}_{-0.0061-0.012}$	$0.302^{+0.0073+0.015}_{-0.0073-0.014}$	$0.298^{+0.0048+0.010}_{-0.0054-0.0092}$
H_0	$67.27^{+0.61+1.20}_{-0.60-1.20}$	$67.68^{+0.45+0.91}_{-0.44-0.87}$	$68.28^{+0.47+0.96}_{-0.48-0.91}$	$68.35^{+0.55+1.12}_{-0.56-1.11}$	$68.66^{+0.41+0.73}_{-0.38-0.76}$
χ^2	2773.168	2779.690	3294.578	2791.542	3318.602

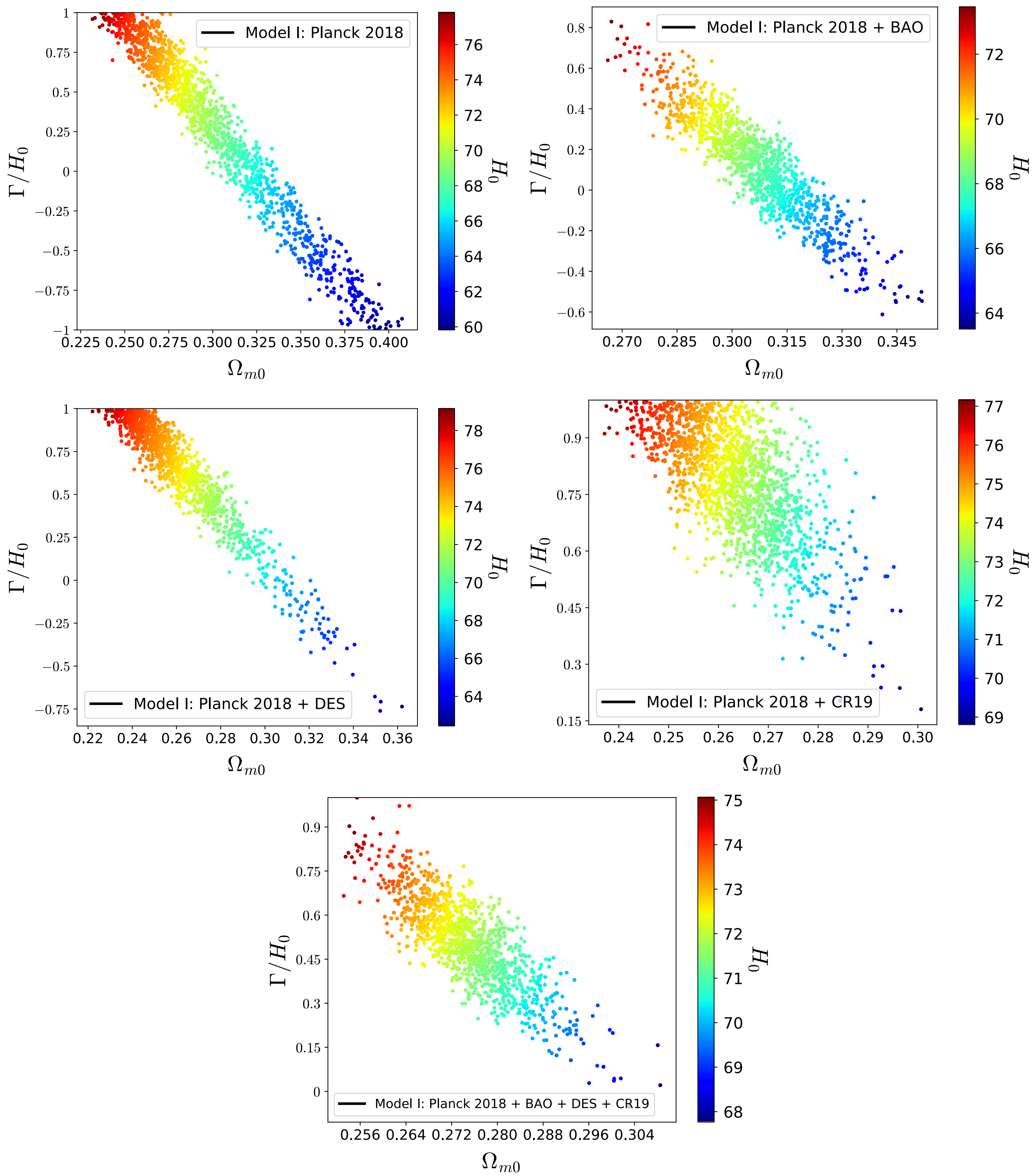

FIG. 4. 3D scattered plots at 95% CL in the plane Γ/H_0 vs Ω_{m0}, coloured by the Hubble constant value H_0 for Model I. A strong anticorrelation between Γ/H_0 and Ω_{m0}, and a positive correlation between Γ/H_0 and H_0 are present. For *Planck* alone, upper left panel, Γ/H_0 is unconstrained, while the addition of external datasets to *Planck* 2018 helps in constraining this parameter.

B. Model II

The results of the observational constraints for the second model of our analysis; that is, for Model II, are shown in Table IV and in Fig. 6. In Fig. 6, for some of the key parameters of this model we show their one-dimensional posterior distributions and the 2-dimensional joint contours at 68% and 95% C.L.

For *Planck* 2018 alone we find an indication of a Γ/H_0 different from zero at more than 1σ. In fact, we have the upper limit $\Gamma/H_0 < -0.39$ at 68% C.L. This clearly shows that the transfer of energy from DM to DE is preferred by *Planck* 2018 data. However, at 2σ, $\Gamma = 0$ is back in agreement with the data. On the other hand, from Fig. 6 we find a strong anticorrelation between H_0 and Γ/H_0, thus, as

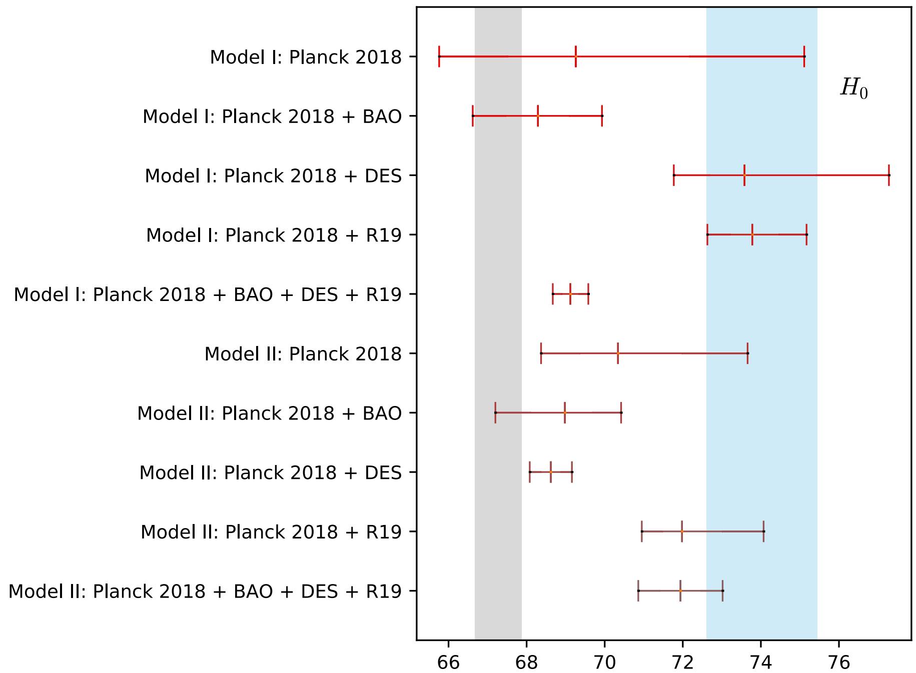

FIG. 5. Whisker plot with 68% CL constraints on H_0 for the metastable DE models (Model I and Model II) for various observational datasets use here. The grey vertical band corresponds to the estimation of H_0 by the final *Planck* 2018 release [1] and the sky blue vertical band corresponds to the R19 value of H_0, as measured by the SH0ES collaboration in [25].

long as Γ/H_0 decreases, H_0 should increase. This fact is reflected by the Hubble constant constraint $H_0 = 70.3^{+3.3}_{-2.0}$ (68% C.L.), which clearly shows that the tension on H_0 between *Planck* 2018 and R19 is solved within 2 standard deviation. Moreover, for this model, because of the flow of energy from DM to DE, we find a lower estimation of cold dark matter ($\Omega_{m0} = 0.18^{+0.07}_{-0.13}$ at 68% C.L.) than its estimation within the ΛCDM model as obtained by *Planck* 2018 in [1]. This is clearly expected for the geometrical degeneracy present in the CMB data: if we have less dark matter, we see a shift of the acoustic peaks and we need a larger H_0 value to have them back in the original position.

When BAO data are added to *Planck* 2018, thanks to the robust constraint BAO data give on the matter density Ω_{m0}, we find that Ω_{m0} slightly increases with respect to the *Planck* 2018 alone case ($\Omega_{m0} = 0.242^{+0.079}_{-0.063}$ at 68% C.L.), but it is still lower than the *Planck* 2018 value in the context of ΛCDM model [1]. Due to the positive

TABLE IV. Summary of the observational constraints and upper limits at 68% and 95% CL on the cosmological scenario driven by the metastable DE scenario, *Model II*, using different observational datasets. The parameters are varying in the ranges described in Table I.

Parameters	*Planck* 2018	*Planck* 2018 + BAO	*Planck* 2018 + DES	*Planck* 2018 + R19	*Planck* 2018 + BAO + DES + R19
$\Omega_c h^2$	$0.064^{+0.022}_{-0.062} < 0.134$	$0.091^{+0.034+0.051}_{-0.023-0.056}$	$0.0998^{+0.0071+0.015}_{-0.0077-0.014}$	$< 0.050 < 0.099$	$0.0983^{+0.0079+0.0153}_{-0.0090-0.0142}$
$\Omega_b h^2$	$0.02231^{+0.00015+0.00030}_{-0.00015-0.00031}$	$0.02233^{+0.00014+0.00028}_{-0.00014-0.00028}$	$0.02237^{+0.00015+0.00029}_{-0.00015-0.00029}$	$0.02236^{+0.00014+0.00030}_{-0.00016-0.00028}$	$0.02246^{+0.00013+0.00026}_{-0.00013-0.00026}$
$100\theta_{MC}$	$1.0444^{+0.0031+0.0049}_{-0.0033-0.0049}$	$1.0425^{+0.0012+0.0037}_{-0.0022-0.0032}$	$1.04183^{+0.00050+0.00095}_{-0.00049-0.00101}$	$1.0461^{+0.0031+0.0039}_{-0.0017-0.0046}$	$1.04202^{+0.00057+0.00101}_{-0.00052-0.00101}$
τ	$0.054^{+0.0075+0.016}_{-0.0077-0.015}$	$0.055^{+0.0076+0.016}_{-0.0081-0.015}$	$0.055^{+0.0077+0.016}_{-0.0076-0.016}$	$0.055^{+0.0071+0.016}_{-0.0081-0.015}$	$0.058^{+0.0074+0.016}_{-0.0077-0.015}$
n_s	$0.9724^{+0.0040+0.0082}_{-0.0042-0.0081}$	$0.9736^{+0.0039+0.0079}_{-0.0039-0.0079}$	$0.9739^{+0.0041+0.0081}_{-0.0040-0.0083}$	$0.9740^{+0.0041+0.0083}_{-0.0041-0.0082}$	$0.9761^{+0.0038+0.0068}_{-0.0037-0.0071}$
$\ln(10^{10}A_s)$	$3.055^{+0.016+0.033}_{-0.016-0.033}$	$3.056^{+0.015+0.032}_{-0.016-0.032}$	$3.056^{+0.015+0.033}_{-0.017-0.032}$	$3.056^{+0.015+0.032}_{-0.015-0.030}$	$3.059^{+0.016+0.033}_{-0.016-0.031}$
Γ/H_0	$< -0.39 < 0.19$	$-0.29^{+0.30+0.54}_{-0.28-0.53}$	$-0.219^{+0.082+0.17}_{-0.090-0.17}$	$< -0.66 < -0.21$	$-0.219^{+0.089+0.174}_{-0.099-0.160}$
Ω_{m0}	$0.18^{+0.07+0.19}_{-0.13-0.16}$	$0.242^{+0.079+0.13}_{-0.063-0.14}$	$0.261^{+0.017+0.038}_{-0.019-0.034}$	$0.127^{+0.031+0.140}_{-0.084-0.098}$	$0.254^{+0.018+0.038}_{-0.023-0.035}$
H_0	$70.3^{+3.3+4.3}_{-2.0-4.9}$	$69.0^{+1.4+3.1}_{-1.8-3.0}$	$68.62^{+0.54+1.1}_{-0.54-1.1}$	$72.0^{+2.1+2.7}_{-1.0-3.4}$	$69.12^{+0.46+0.83}_{-0.45-0.86}$
χ^2	2771.716	2780.014	3295.094	2775.360	3315.868

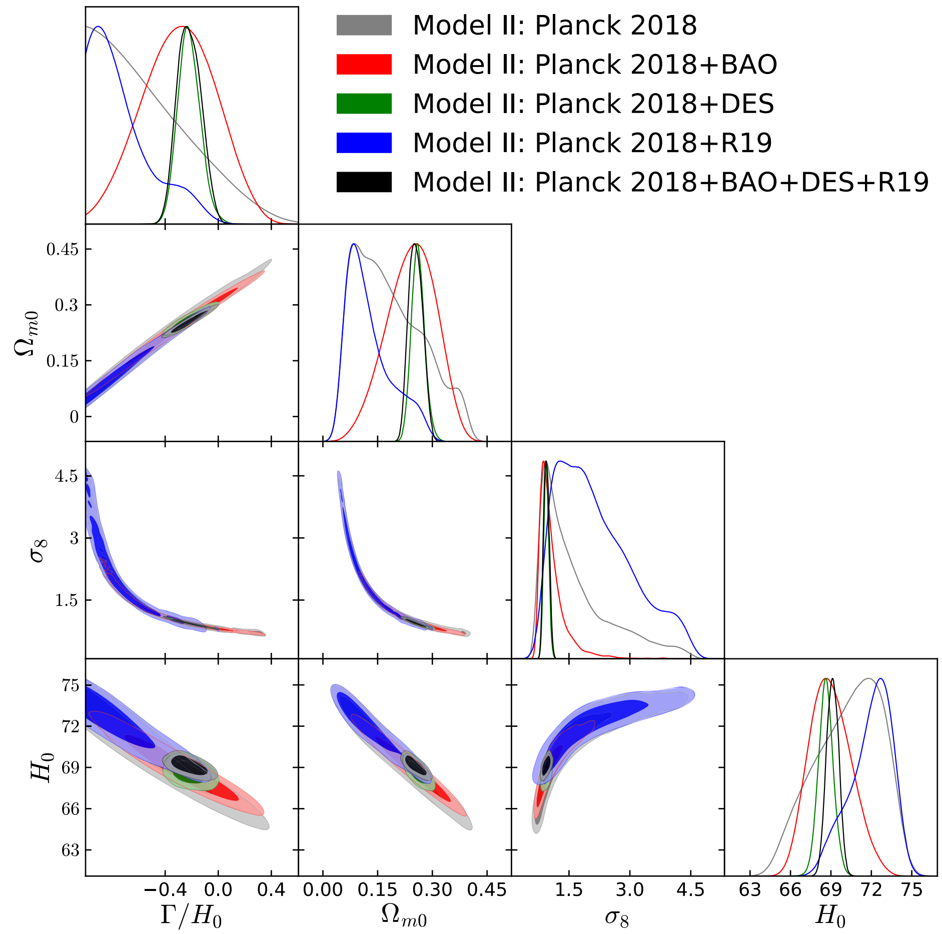

FIG. 6. 68% and 95% CL constraints on the metastable DE scenario, *Model II*, using various observational datasets have been displayed.

correlation between Ω_{m0} and Γ/H_0, as we can see from Figs. 7 and 6, we find that Γ/H_0 is in agreement with the zero value within one standard deviation. This means that Γ/H_0, i.e., the rate of energy transfer between the dark sectors, is in agreement with the expected value in the ΛCDM model. Hence, because of the very well known anticorrelation between Ω_{m0} and H_0, we see that the Hubble constant shifts toward lower value compared to its estimation from *Planck* 2018 alone, and moreover, its error bars are significantly decreased. Thus, the tension on H_0 slightly increases at 2.5σ, but of course it is always less than the 4.4σ tension between *Planck* 2018 [1] and the SH0ES collaboration [25] within the ΛCDM scenario. Moreover, because of the extraction method, the BAO data are not completely reliable in fitting extended DE models, as already pointed out in [72].

We continue by considering the next two datasets *Planck* 2018 + DES and *Planck* 2018 + R19. For both cases since the tension between the datasets (*Planck* 2018, DES) and (*Planck* 2018, R19) is solved in this scenario, we can safely combine them, that means, we can consider the combined analysis *Planck* 2018 + DES and *Planck* 2018 + R19. The results for *Planck* 2018 + DES and *Planck* 2018 + R19 are shown in the last two columns of Table IV. For *Planck* 2018 + DES we remark a really strong bound on Γ/H_0, which is lower than zero at more than 2σ and very well constrained. Since Γ/H_0 takes larger values than *Planck* 2018 and *Planck* 2018 + BAO, and as we observe in Fig. 7 for the three parameter correlation, it follows a slightly larger value of Ω_{m0} and a smaller value of H_0 with respect to the previous cases. For this reason the Hubble constant tension with R19 is restored in this scenario at about 3.6σ. For *Planck* 2018 + R19 we find a very strong upper limit on Γ/H_0, that is less than zero at several standard deviations. That means essentially we have an increasing DE scenario for this metastable DE model. Concerning Ω_{m0} estimations, similarly to the previous cases, the matter density again decreases.

Finally, we combined all the datasets and showed the results in the last column of Table IV. Our results are similar to what we have observed with *Planck* 2018 + DES. That means an indication of negative value of Γ/H_0 is supported by the combined data.

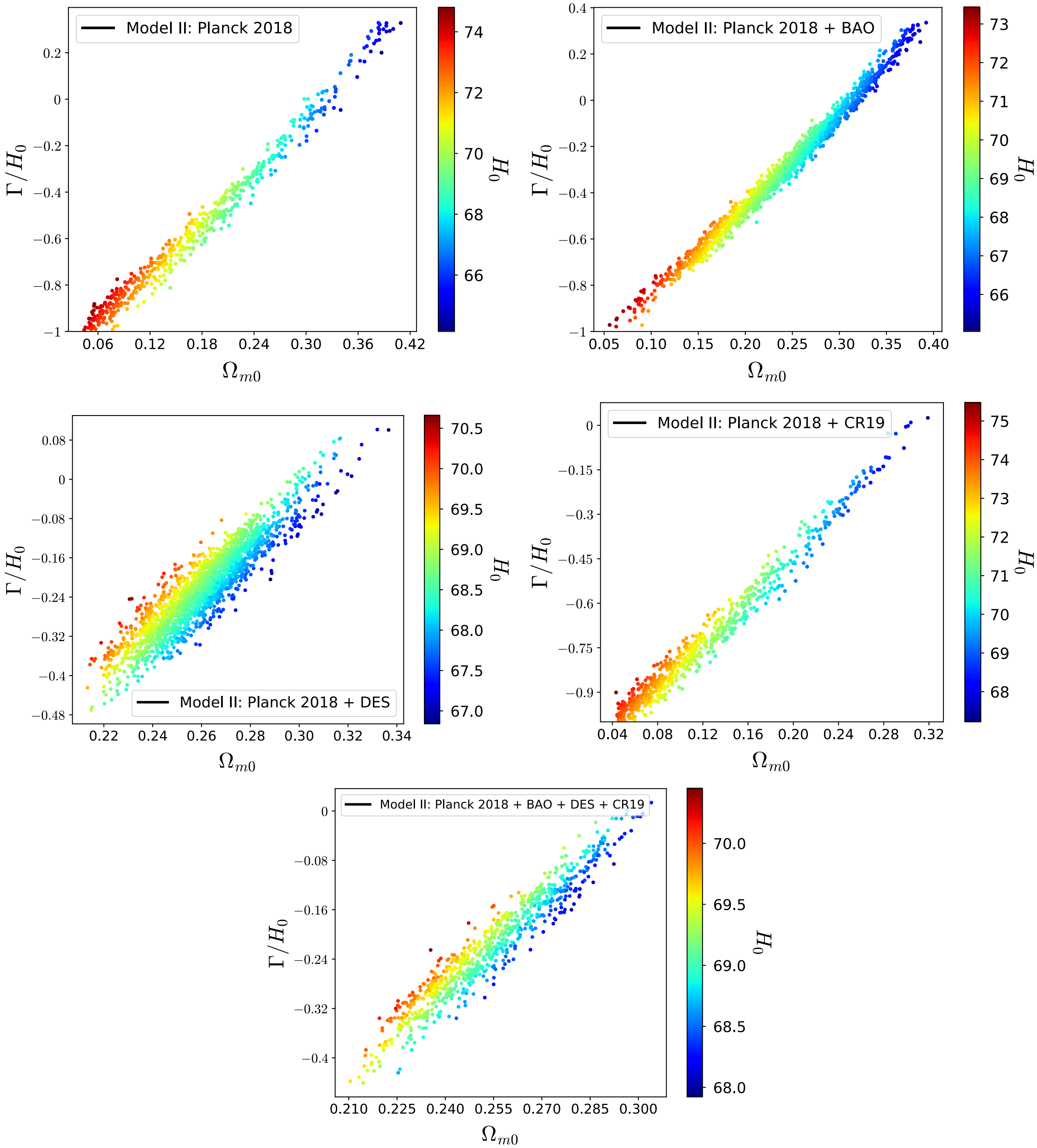

FIG. 7. 3D scattered plots at 95% CL in the plane Γ/H_0 vs Ω_{m0}, colored by the Hubble constant value H_0 for Model II. On the contrary of Model I, a strong positive correlation between Γ/H_0 and Ω_{m0}, and a negative correlation between Γ/H_0 and H_0 are present.

We refer to Fig. 5 showing the whisker plot of H_0 at 68% CL with its measurements by different observational data. The whisker plot in Fig. 5 clearly shows how the tension on H_0 is alleviated for most of the data combination, with the exception of *Planck* 2018 + DES. In summary, within this metastable DE scenario, the energy density of DE is increasing, as reported by the observational data preferring a negative value for Γ/H_0.

V. SUMMARY AND CONCLUDING REMARKS

In this work we have investigated two metastable DE models by considering their evolution at the level of linear perturbations and constrain their parameter space in light of the latest observational data with a special focus on the CMB data from *Planck* 2018. The consideration of perturbation equations is one of the main ingredients of our work and therefore the present article generalizes earlier publications of [94,95] where the perturbation equations of the metastable DE models were not considered. Since the early time instability of any dark energy model can be visualized directly by investigating its equations at the perturbative level implies that the inclusion of the perturbations equations are essential in understanding the actual dynamics of the DE model. Additionally, there is a relation between the observational constraints of the explored models and the dynamical level, that means, whether the dynamics of the model is considered at the background level or at background plus perturbative levels. Concerning the observational data, we use the full CMB measurements from final *Planck* 2018 release [115,116], BAO [189–191], DES [47,48,192] and a measurement of H_0 from SH0ES collaboration (R19) [25]. In order to investigate the present models, we have considered the following datasets and their combinations: *Planck* 2018 alone, *Planck* 2018 + BAO, *Planck* 2018 + DES and *Planck* 2018 + R19. The inclusion of BAO to CMB is used to break the degeneracies between the parameters. For the last two cases, i.e., 2018 + DES and *Planck* 2018 + R19, the combination of *Planck* 2018 to either DES or R19 is possible since the tensions between these datasets are solved within these models.

For the first metastable DE model (4), we have summarized the results in Table II and in Figs. 3 and 4. We remark that for all datasets we find $\Gamma/H_0 > 0$ which indicates that DE has a decaying nature within this context. While we mention that for *Planck* 2018 alone, Γ/H_0 remains positive at about 68% CL, such evidence becomes stronger for the following combinations *Planck* 2018 + DES and *Planck* 2018 + R19. However, for *Planck* 2018 + BAO, $\Gamma = 0$ is consistent within 68% CL. Additionally, we found that within this model, the tension on H_0 is mostly solved. Specifically, we notice that for *Planck* 2018 data alone, *Planck* 2018 + DES, and *Planck* 2018 + R19, the tension on H_0 is significantly alleviated within 1σ. However, for *Planck* 2018 + BAO, the tension on H_0 is just reduced at 2.6σ (see Fig. 5 for a better understanding).

The results of the second metastable DE model are shown in Table IV and Fig. 6. From the results, one can clearly conclude that, within this model scenario, $\Gamma/H_0 < 0$ is preferred for all the data combination, with the exception of *Planck* 2018 + BAO where $\Gamma = 0$ is consistent within 68% C.L. So, for most of the observational data, an increasing of DE density (i.e., DM decays into DE) is favored. The tension on H_0 is alleviated for *Planck* 2018 within 2σ. However, for *Planck* 2018 + BAO it is weakened at 2.5σ and for *Planck* 2018 + R19 it is completely solved.

Concerning the earlier publications of [94,95], the main improvements of the present work can be seen as follows. First the inclusion of the perturbation equations of the metastable DE models generalizes the work of [94,95] and second the present work employs the CMB full likelihood analysis compared to those of [94,95] where the CMB distance priors were used. These differences naturally introduce some differences as far as the observational constraints are concerned, especially on the estimation of the Hubble constant, H_0. We believe that our work offers a very transparent picture in alleviating the so called Hubble constant tension. In fact, from Figs. 1 and 2 one can understand how the models behave on large scales. In particular, Fig. 2 clearly demonstrates how the coupling parameter plays an important role in order to quantify the behavior of Model II on large scales.

Thus, based on the observational data considered in this work and the results, specifically, focusing on the nonzero values of Γ/H_0 obtained from the presently used datasets, one may strongly argue that the metastable DE models should be investigated further with more data points, see for instance the updated data points in [188] as well as the upcoming observational datasets in order to arrive at a definite conclusion regarding their viabilities. Moreover, as we have found that the metastable DE models with just an additional extra free parameter Γ/H_0 can solve quite efficiently the Hubble constant tension.

Last but not least, we would like to emphasize that the choice of the metastable DE models is not unique. Since the nature of DE is not purely understood, thus, there is no reason to exclude other metastable DE models beyond the present choices. For instance, some alternatives to the exponential choice of Model I can be considered. In a similar way, one could also generalize Model II by considering other functional forms. Although Model II describes an interacting scenario and similar choices are available in the literature; however, the exact functional form of the interaction rate is not yet revealed. Hence, we believe that metastable DE models should gain significant attention in the cosmological community due to the fact that within such models, the extrinsic properties of the universe do not come into the picture, only the intrinsic nature of DE plays the master role.

ACKNOWLEDGMENTS

The authors are grateful to the referees for their comments and suggestions that improved the quality of the manuscript. W. Y. has been supported by the National Natural Science Foundation of China under Grants No. 11705079 and No. 11647153. E. D. V. acknowledges support from the European Research Council in the form of a Consolidator Grant with No. 681431. S. P. has been supported by the Mathematical Research Impact-Centric Support Scheme (MATRICS), File No. MTR/2018/000940, given by the Science and Engineering Research Board (SERB), Govt. of India. S. B. acknowledges support from the Research Center for Astronomy of the Academy of Athens in the context of the program *Tracing the Cosmic Acceleration*.

[1] N. Aghanim *et al.* (Planck Collaboration), Planck 2018 results. VI. Cosmological parameters, arXiv:1807.06209.

[2] J. R. Gott, M. S. Vogeley, S. Podariu, and B. Ratra, Median statistics, H(0), and the accelerating universe, Astrophys. J. **549**, 1 (2001).

[3] G. Chen and B. Ratra, Median statistics and the Hubble constant, Publ. Astron. Soc. Pac. **123**, 1127 (2011).

[4] G. Efstathiou, H0 revisited, Mon. Not. R. Astron. Soc. **440**, 1138 (2014).

[5] Y. Chen, S. Kumar, and B. Ratra, Determining the Hubble constant from Hubble parameter measurements, Astrophys. J. **835**, 86 (2017).

[6] Y. Wang, L. Xu, and G. B. Zhao, A measurement of the Hubble constant using galaxy redshift surveys, Astrophys. J. **849**, 84 (2017).

[7] W. Lin and M. Ishak, Cosmological discordances II: Hubble constant, Planck and large-scale-structure data sets, Phys. Rev. D **96**, 083532 (2017).

[8] H. Yu, B. Ratra, and F. Y. Wang, Hubble parameter and Baryon acoustic oscillation measurement constraints on the Hubble constant, the deviation from the spatially flat ΛCDM model, the deceleration-acceleration transition redshift, and spatial curvature, Astrophys. J. **856**, 3 (2018).

[9] T. Abbott *et al.* (DES Collaboration), Dark energy survey year 1 results: A precise H0 estimate from DES Y1, BAO, and D/H data, Mon. Not. R. Astron. Soc. **480**, 3879 (2018).

[10] B. S. Haridasu, V. V. Luković, M. Moresco, and N. Vittorio, An improved model-independent assessment of the late-time cosmic expansion, J. Cosmol. Astropart. Phys. 10 (2018) 015.

[11] J. Zhang, Most frequent value statistics and the Hubble constant, Publ. Astron. Soc. Pac. **130**, 084502 (2018).

[12] C. G. Park and B. Ratra, Measuring the Hubble constant and spatial curvature from supernova apparent magnitude, baryon acoustic oscillation, and Hubble parameter data, Astrophys. Space Sci. **364**, 134 (2019).

[13] X. Zhang and Q. G. Huang, Constraints on H_0 from WMAP and BAO measurements, Commun. Theor. Phys. **71**, 826 (2019).

[14] J. Ryan, Y. Chen, and B. Ratra, Baryon acoustic oscillation, Hubble parameter, and angular size measurement constraints on the Hubble constant, dark energy dynamics, and spatial curvature, Mon. Not. R. Astron. Soc. **488**, 3844 (2019).

[15] A. Domínguez, R. Wojtak, J. Finke, M. Ajello, K. Helgason, F. Prada, A. Desai, V. Paliya, L. Marcotulli, and D. H. Hartmann, A new measurement of the Hubble constant and matter content of the Universe using extragalactic background light γ-ray attenuation, Astrophys. J. **885**, 137 (2019).

[16] A. Cuceu, J. Farr, P. Lemos, and A. Font-Ribera, Baryon acoustic oscillations and the Hubble constant: Past, present and future, J. Cosmol. Astropart. Phys. 10 (2019) 044.

[17] V. V. Luković, B. S. Haridasu, and N. Vittorio, Exploring the evidence for a large local void with supernovae Ia data, Mon. Not. R. Astron. Soc. **491**, 2075 (2020).

[18] H. Zeng and D. Yan, Using the extragalactic Gamma-ray background to constrain the Hubble constant and matter density of the Universe, Astrophys. J. **882**, 87 (2019).

[19] W. Lin and M. Ishak, Remarks on measures of inconsistency, arXiv:1909.10991.

[20] W. L. Freedman *et al.*, The Carnegie-Chicago Hubble program. VIII. An independent determination of the Hubble constant based on the tip of the red giant branch, Astrophys. J. **882**, 34 (2019).

[21] W. L. Freedman, B. F. Madore, T. Hoyt, I. S. Jang, R. Beaton, M. G. Lee, A. Monson, J. Neeley, and J. Rich, Calibration of the tip of the red giant branch (TRGB), Astrophys. J. **891**, 57 (2020).

[22] S. Cao, J. Ryan, and B. Ratra, Cosmological constraints from HII starburst galaxy apparent magnitude and other cosmological measurements, Mon. Not. R. Astron. Soc. **497**, 3191 (2020).

[23] S. Alam *et al.* (eBOSS Collaboration), The completed SDSS-IV extended Baryon oscillation spectroscopic survey: Cosmological implications from two decades of spectroscopic surveys at the Apache point observatory, arXiv:2007.08991.

[24] S. Birrer *et al.*, TDCOSMO IV: Hierarchical time-delay cosmography–Joint inference of the Hubble constant and galaxy density profiles, arXiv:2007.02941.

[25] A. G. Riess, S. Casertano, W. Yuan, L. M. Macri, and D. Scolnic, Large magellanic cloud Cepheid standards provide a 1% foundation for the determination of the Hubble constant and stronger evidence for physics beyond ΛCDM, Astrophys. J. **876**, 85 (2019).

[26] M. Rigault *et al.*, Confirmation of a star formation bias in Type Ia Supernova distances and its effect on measurement of the Hubble constant, Astrophys. J. **802**, 20 (2015).

[27] W. Cardona, M. Kunz, and V. Pettorino, Determining H_0 with Bayesian hyper-parameters, J. Cosmol. Astropart. Phys. 03 (2017) 056.

[28] A. G. Riess *et al.*, A 2.4% determination of the local value of the Hubble constant, Astrophys. J. **826**, 56 (2016).

[29] B. R. Zhang, M. J. Childress, T. M. Davis, N. V. Karpenka, C. Lidman, B. P. Schmidt, and M. Smith, A blinded determination of H_0 from low-redshift Type Ia supernovae, calibrated by Cepheid variables, Mon. Not. R. Astron. Soc. **471**, 2254 (2017).

[30] S. Dhawan, S. W. Jha, and B. Leibundgut, Measuring the Hubble constant with Type Ia Supernovae as near-infrared standard candles, Astron. Astrophys. **609**, A72 (2018).

[31] D. Fernández Arenas, E. Terlevich, R. Terlevich, J. Melnick, R. Chávez, F. Bresolin, E. Telles, M. Plionis, and S. Basilakos, An independent determination of the local Hubble constant, Mon. Not. R. Astron. Soc. **474**, 1250 (2018).

[32] S. Birrer *et al.*, H0LiCOW—IX. Cosmographic analysis of the doubly imaged quasar SDSS 1206 + 4332 and a new measurement of the Hubble constant, Mon. Not. R. Astron. Soc. **484**, 4726 (2019).

[33] A. G. Riess *et al.*, New parallaxes of Galactic Cepheids from spatially scanning the Hubble space telescope: Implications for the Hubble constant, Astrophys. J. **855**, 136 (2018).

[34] D. Camarena and V. Marra, Local determination of the Hubble constant and the deceleration parameter, Phys. Rev. Research **2**, 013028 (2020).

[35] K. C. Wong *et al.*, H0LiCOW XIII. A 2.4% measurement of H_0 from lensed quasars: 5.3σ tension between early and late-Universe probes, arXiv:1907.04869 [Mon. Not. R. Astron. Soc. (to be published)].
[36] W. Yuan, A. G. Riess, L. M. Macri, S. Casertano, and D. Scolnic, Consistent calibration of the tip of the red giant branch in the large magellanic cloud on the Hubble space telescope photometric system and a re-determination of the Hubble constant, Astrophys. J. **886**, 61 (2019).
[37] C. D. Huang, A. G. Riess, W. Yuan, L. M. Macri, N. L. Zakamska, S. Casertano, P. A. Whitelock, S. L. Hoffmann, A. V. Filippenko, and D. Scolnic, Hubble space telescope observations of Mira variables in the Type Ia Supernova host NGC 1559: An alternative candle to measure the Hubble constant, Astrophys. J. **889**, 5 (2020).
[38] A. Shajib *et al.* (DES Collaboration), STRIDES: A 3.9 per cent measurement of the Hubble constant from the strong lens system DES J0408-5354, Mon. Not. R. Astron. Soc. **494**, 6072 (2020).
[39] L. Verde, T. Treu, and A. Riess, Tensions between the early and the late universe, Nat. Astron. **3**, 891 (2019).
[40] J. W. Henning *et al.* (SPT Collaboration), Measurements of the temperature and e-mode polarization of the CMB from 500 square degrees of SPTpol data, Astrophys. J. **852**, 97 (2018).
[41] M. J. Reid, D. W. Pesce, and A. G. Riess, An improved distance to NGC 4258 and its implications for the Hubble constant, Astrophys. J. Lett. **886**, L27 (2019).
[42] G. Efstathiou, A lockdown perspective on the Hubble tension (with comments from the SH0ES team), arXiv: 2007.10716.
[43] D. W. Pesce, J. A. Braatz, M. J. Reid, A. G. Riess, D. Scolnic, J. J. Condon, F. Gao, C. Henkel, C. M. V. Impellizzeri, C. Y. Kuo, and K. Y. Lo, The megamaser cosmology project. XIII. Combined Hubble constant constraints, Astrophys. J. Lett. **891**, L1 (2020).
[44] K. Kuijken *et al.*, Gravitational lensing analysis of the Kilo Degree Survey, Mon. Not. R. Astron. Soc. **454**, 3500 (2015).
[45] H. Hildebrandt *et al.*, KiDS-450: Cosmological parameter constraints from tomographic weak gravitational lensing, Mon. Not. R. Astron. Soc. **465**, 1454 (2017).
[46] I. Fenech Conti, R. Herbonnet, H. Hoekstra, J. Merten, L. Miller, and M. Viola, Calibration of weak-lensing shear in the Kilo-Degree Survey, Mon. Not. R. Astron. Soc. **467**, 1627 (2017).
[47] M. A. Troxel *et al.* (DES Collaboration), Dark energy survey year 1 results: Cosmological constraints from cosmic shear, Phys. Rev. D **98**, 043528 (2018).
[48] T. M. C. Abbott *et al.* (DES Collaboration), Dark energy survey year 1 results: Cosmological constraints from Galaxy clustering and weak lensing, Phys. Rev. D **98**, 043526 (2018).
[49] C. Heymans *et al.*, CFHTLenS: The Canada-France-Hawaii telescope lensing survey, Mon. Not. R. Astron. Soc. **427**, 146 (2012).
[50] T. Erben *et al.*, CFHTLenS: The Canada-France-Hawaii telescope lensing survey—Imaging data and catalogue products, Mon. Not. R. Astron. Soc. **433**, 2545 (2013).
[51] S. Joudaki *et al.*, CFHTLenS revisited: Assessing concordance with Planck including astrophysical systematics, Mon. Not. R. Astron. Soc. **465**, 2033 (2017).
[52] E. Di Valentino, A. Melchiorri, and J. Silk, Planck evidence for a closed Universe and a possible crisis for cosmology, Nat. Astron. **4**, 196 (2019).
[53] E. Di Valentino, A. Melchiorri, and J. Silk, Beyond six parameters: Extending ΛCDM, Phys. Rev. D **92**, 121302 (2015).
[54] E. Di Valentino, A. Melchiorri, and J. Silk, Reconciling Planck with the local value of H_0 in extended parameter space, Phys. Lett. B **761**, 242 (2016).
[55] E. Di Valentino, A. Melchiorri, E. V. Linder, and J. Silk, Constraining dark energy dynamics in extended parameter space, Phys. Rev. D **96**, 023523 (2017).
[56] E. Di Valentino, A. Melchiorri, and J. Silk, Cosmological constraints in extended parameter space from the Planck 2018 Legacy release, J. Cosmol. Astropart. Phys. 01 (2020) 013.
[57] E. Di Valentino, A. Melchiorri, and J. Silk, Cosmic discordance: Planck and luminosity distance data exclude LCDM, arXiv:2003.04935.
[58] V. Pettorino, L. Amendola, and C. Wetterich, How early is early dark energy?, Phys. Rev. D **87**, 083009 (2013).
[59] V. Poulin, T. L. Smith, T. Karwal, and M. Kamionkowski, Early Dark Energy Can Resolve the Hubble Tension, Phys. Rev. Lett. **122**, 221301 (2019).
[60] S. Alexander and E. McDonough, Axion-dilaton destabilization and the Hubble tension, Phys. Lett. B **797**, 134830 (2019).
[61] J. Sakstein and M. Trodden, Early Dark Energy from Massive Neutrinos—A Natural Resolution of the Hubble Tension, Phys. Rev. Lett. **124**, 161301 (2020).
[62] F. Niedermann and M. S. Sloth, New early dark energy, arXiv:1910.10739.
[63] G. Ye and Y. S. Piao, Is the Hubble tension a hint of AdS phase around recombination?, Phys. Rev. D **101**, 083507 (2020).
[64] S. Kumar and R. C. Nunes, Probing the interaction between dark matter and dark energy in the presence of massive neutrinos, Phys. Rev. D **94**, 123511 (2016).
[65] S. Kumar and R. C. Nunes, Echo of interactions in the dark sector, Phys. Rev. D **96**, 103511 (2017).
[66] E. Di Valentino, A. Melchiorri, and O. Mena, Can interacting dark energy solve the H_0 tension? Phys. Rev. D **96**, 043503 (2017).
[67] W. Yang, S. Pan, E. Di Valentino, R. C. Nunes, S. Vagnozzi, and D. F. Mota, Tale of stable interacting dark energy, observational signatures, and the H_0 tension, J. Cosmol. Astropart. Phys. 09 (2018) 019.
[68] W. Yang, A. Mukherjee, E. Di Valentino, and S. Pan, Interacting dark energy with time varying equation of state and the H_0 tension, Phys. Rev. D **98**, 123527 (2018).
[69] W. Yang, O. Mena, S. Pan, and E. Di Valentino, Dark sectors with dynamical coupling, Phys. Rev. D **100**, 083509 (2019).
[70] M. Martinelli, N. B. Hogg, S. Peirone, M. Bruni, and D. Wands, Constraints on the interacting vacuum—geodesic CDM scenario, Mon. Not. R. Astron. Soc. **488**, 3423 (2019).

[71] E. Di Valentino, A. Melchiorri, O. Mena, and S. Vagnozzi, Interacting dark energy after the latest Planck, DES, and H_0 measurements: An excellent solution to the H_0 and cosmic shear tensions, Phys. Dark Universe **30**, 100666 (2020).

[72] E. Di Valentino, A. Melchiorri, O. Mena, and S. Vagnozzi, Nonminimal dark sector physics and cosmological tensions, Phys. Rev. D **101**, 063502 (2020).

[73] E. Di Valentino, S. Gariazzo, O. Mena, and S. Vagnozzi, Soundness of dark energy properties, J. Cosmol. Astropart. Phys. 07 (2020) 045.

[74] M. Raveri, Reconstructing gravity on cosmological scales, Phys. Rev. D **101**, 083524 (2020).

[75] S. F. Yan, P. Zhang, J. W. Chen, X. Z. Zhang, Y. F. Cai, and E. N. Saridakis, Interpreting cosmological tensions from the effective field theory of torsional gravity, Phys. Rev. D **101**, 121301 (2020).

[76] N. Frusciante, S. Peirone, L. Atayde, and A. De Felice, Phenomenology of the generalized cubic covariant Galileon model and cosmological bounds, Phys. Rev. D **101**, 064001 (2020).

[77] E. Di Valentino, C. Bøehm, E. Hivon, and F. R. Bouchet, Reducing the H_0 and σ_8 tensions with dark matter-neutrino interactions, Phys. Rev. D **97**, 043513 (2018).

[78] E. Di Valentino, E. V. Linder, and A. Melchiorri, Vacuum phase transition solves the H_0 tension, Phys. Rev. D **97**, 043528 (2018).

[79] N. Khosravi, S. Baghram, N. Afshordi, and N. Altamirano, H_0 tension as a hint for a transition in gravitational theory, Phys. Rev. D **99**, 103526 (2019).

[80] J. Renk, M. Zumalacárregui, F. Montanari, and A. Barreira, Galileon gravity in light of ISW, CMB, BAO and H_0 data, J. Cosmol. Astropart. Phys. 10 (2017) 020.

[81] E. Di Valentino, Crack in the cosmological paradigm, Nat. Astron. **1**, 569 (2017).

[82] J. Solà, A. Gómez-Valent, and J. de Cruz Pérez, The H_0 tension in light of vacuum dynamics in the Universe, Phys. Lett. B **774**, 317 (2017).

[83] R. C. Nunes, Structure formation in $f(T)$ gravity and a solution for H_0 tension, J. Cosmol. Astropart. Phys. 05 (2018) 052.

[84] F. D'Eramo, R. Z. Ferreira, A. Notari, and J. L. Bernal, Hot axions and the H_0 tension, J. Cosmol. Astropart. Phys. 11 (2018) 014.

[85] R. Y. Guo, J. F. Zhang, and X. Zhang, Can the H_0 tension be resolved in extensions to ΛCDM cosmology? J. Cosmol. Astropart. Phys. 02 (2019) 054.

[86] W. Yang, S. Pan, E. Di Valentino, E. N. Saridakis, and S. Chakraborty, Observational constraints on one-parameter dynamical dark-energy parametrizations and the H_0 tension, Phys. Rev. D **99**, 043543 (2019).

[87] A. Banihashemi, N. Khosravi, and A. H. Shirazi, Ups and downs in dark energy: Phase transition in dark sector as a proposal to lessen cosmological tensions, Phys. Rev. D **101**, 123521 (2020).

[88] E. Ó Colgáin, M. H. P. M. van Putten, and H. Yavartanoo, de Sitter Swampland, H_0 tension & observation, Phys. Lett. B **793**, 126 (2019).

[89] A. Banihashemi, N. Khosravi, and A. H. Shirazi, Ginzburg-Landau theory of dark energy: A framework to study both temporal and spatial cosmological tensions simultaneously, Phys. Rev. D **99**, 083509 (2019).

[90] C. D. Kreisch, F. Y. Cyr-Racine, and O. Doré, The neutrino puzzle: Anomalies, interactions, and cosmological tensions, Phys. Rev. D **101**, 123505 (2020).

[91] E. Di Valentino, R. Z. Ferreira, L. Visinelli, and U. Danielsson, Late time transitions in the quintessence field and the H_0 tension, Phys. Dark Universe **26**, 100385 (2019).

[92] L. Visinelli, S. Vagnozzi, and U. Danielsson, Revisiting a negative cosmological constant from low-redshift data, Symmetry **11**, 1035 (2019).

[93] N. Schöneberg, J. Lesgourgues, and D. C. Hooper, The BAO + BBN take on the Hubble tension, J. Cosmol. Astropart. Phys. 10 (2019) 029.

[94] A. Shafieloo, D. K. Hazra, V. Sahni, and A. A. Starobinsky, Metastable dark energy with radioactive-like decay, Mon. Not. R. Astron. Soc. **473**, 2760 (2018).

[95] X. Li, A. Shafieloo, V. Sahni, and A. A. Starobinsky, Revisiting metastable dark energy and tensions in the estimation of cosmological parameters, Astrophys. J. **887**, 153 (2019).

[96] M. Martinelli and I. Tutusaus, CMB tensions with low-redshift H_0 and S_8 measurements: Impact of a redshift-dependent type-Ia supernovae intrinsic luminosity, Symmetry **11**, 986 (2019).

[97] H. Desmond, B. Jain, and J. Sakstein, Local resolution of the Hubble tension: The impact of screened fifth forces on the cosmic distance ladder, Phys. Rev. D **100**, 043537 (2019).

[98] K. Vattis, S. M. Koushiappas, and A. Loeb, Dark matter decaying in the late Universe can relieve the H0 tension, Phys. Rev. D **99**, 121302 (2019).

[99] S. Kumar, R. C. Nunes, and S. K. Yadav, Dark sector interaction: A remedy of the tensions between CMB and LSS data, Eur. Phys. J. C **79**, 576 (2019).

[100] P. Agrawal, F. Y. Cyr-Racine, D. Pinner, and L. Randall, Rock 'n' Roll solutions to the Hubble tension, arXiv:1904.01016.

[101] W. Yang, S. Pan, A. Paliathanasis, S. Ghosh, and Y. Wu, Observational constraints of a new unified dark fluid and the H_0 tension, Mon. Not. R. Astron. Soc. **490**, 2071 (2019).

[102] W. Yang, S. Pan, E. Di Valentino, A. Paliathanasis, and J. Lu, Challenging bulk viscous unified scenarios with cosmological observations, Phys. Rev. D **100**, 103518 (2019).

[103] W. Yang, S. Pan, S. Vagnozzi, E. Di Valentino, D. F. Mota, and S. Capozziello, Dawn of the dark: Unified dark sectors and the EDGES cosmic dawn 21-cm signal, J. Cosmol. Astropart. Phys. 11 (2019) 044.

[104] S. Pan, W. Yang, E. Di Valentino, E. N. Saridakis, and S. Chakraborty, Interacting scenarios with dynamical dark energy: observational constraints and alleviation of the H_0 tension, Phys. Rev. D **100**, 103520 (2019).

[105] Y. F. Cai, M. Khurshudyan, and E. N. Saridakis, Model-independent reconstruction of $f(T)$ gravity from Gaussian processes, Astrophys. J. **888**, 62 (2020).

[106] S. Pan, W. Yang, E. Di Valentino, A. Shafieloo, and S. Chakraborty, Reconciling H_0 tension in a six parameter space? J. Cosmol. Astropart. Phys. 06 (2020) 062.

[107] E. Ó. Colgáin and H. Yavartanoo, Testing the swampland: H_0 tension, Phys. Lett. B **797**, 134907 (2019).
[108] S. Pan, W. Yang, C. Singha, and E. N. Saridakis, Observational constraints on sign-changeable interaction models and alleviation of the H_0 tension, Phys. Rev. D **100**, 083539 (2019).
[109] K. V. Berghaus and T. Karwal, Thermal friction as a solution to the Hubble tension, Phys. Rev. D **101**, 083537 (2020).
[110] E. Di Valentino, A. Mukherjee, and A. A. Sen, Dark energy with phantom crossing and the H_0 tension, arXiv:2005.12587.
[111] A. Pourtsidou and T. Tram, Reconciling CMB and structure growth measurements with dark energy interactions, Phys. Rev. D **94**, 043518 (2016).
[112] R. An, C. Feng, and B. Wang, Relieving the tension between weak lensing and cosmic microwave background with interacting dark matter and dark energy models, J. Cosmol. Astropart. Phys. 02 (2018) 038.
[113] E. Di Valentino and S. Bridle, Exploring the tension between current cosmic microwave background and cosmic shear data, Symmetry **10**, 585 (2018).
[114] L. Kazantzidis and L. Perivolaropoulos, Evolution of the $f\sigma_8$ tension with the $Planck15/\Lambda$CDM determination and implications for modified gravity theories, Phys. Rev. D **97**, 103503 (2018).
[115] N. Aghanim *et al.* (Planck Collaboration), Planck 2018 results. VIII. Gravitational lensing, arXiv:1807.06210.
[116] N. Aghanim *et al.* (Planck Collaboration), Planck 2018 results. V. CMB power spectra and likelihoods, arXiv:1907.12875.
[117] P. J. E. Peebles and B. Ratra, Cosmology with a time-variable cosmological "constant", Astrophys. J. Lett. **325**, L17 (1988).
[118] B. Ratra and P. Peebles, Cosmological consequences of a rolling homogeneous scalar field, Phys. Rev. D **37**, 3406 (1988).
[119] C. P. Ma and E. Bertschinger, Cosmological perturbation theory in the synchronous and conformal Newtonian gauges, Astrophys. J. **455**, 7 (1995).
[120] W. Hu, Structure formation with generalized dark matter, Astrophys. J. **506**, 485 (1998).
[121] J. Väliviita, E. Majerotto, and R. Maartens, Instability in interacting dark energy and dark matter fluids, J. Cosmol. Astropart. Phys. 07 (2008) 020.
[122] W. Yang, S. Pan, and J. D. Barrow, Large-scale stability and astronomical constraints for coupled dark-energy models, Phys. Rev. D **97**, 043529 (2018).
[123] G. Ballesteros and A. Riotto, Parameterizing the effect of dark energy perturbations on the growth of structures, Phys. Lett. B **668**, 171 (2008).
[124] D. Sapone and E. Majerotto, Fingerprinting dark energy III: Distinctive marks of viscosity, Phys. Rev. D **85**, 123529 (2012).
[125] F. Pace, R. C. Batista, and A. Del Popolo, Effects of shear and rotation on the spherical collapse model for clustering dark energy, Mon. Not. R. Astron. Soc. **445**, 648 (2014).
[126] S. Basilakos, The growth index of matter perturbations using the clustering of dark energy, Mon. Not. R. Astron. Soc. **449**, 2151 (2015).
[127] S. Nesseris and D. Sapone, Accuracy of the growth index in the presence of dark energy perturbations, Phys. Rev. D **92**, 023013 (2015).
[128] A. Mehrabi, S. Basilakos, and F. Pace, How clustering dark energy affects matter perturbations, Mon. Not. R. Astron. Soc. **452**, 2930 (2015).
[129] C. Wetterich, The Cosmon model for an asymptotically vanishing time dependent cosmological 'constant', Astron. Astrophys. **301**, 321 (1995).
[130] L. Amendola, Coupled quintessence, Phys. Rev. D **62**, 043511 (2000).
[131] R. G. Cai and A. Wang, Cosmology with interaction between phantom dark energy and dark matter and the coincidence problem, J. Cosmol. Astropart. Phys. 03 (2005) 002.
[132] S. del Campo, R. Herrera, and D. Pavón, Toward a solution of the coincidence problem, Phys. Rev. D **78**, 021302 (2008).
[133] S. del Campo, R. Herrera, and D. Pavón, Interacting models may be key to solve the cosmic coincidence problem, J. Cosmol. Astropart. Phys. 01 (2009) 020.
[134] W. Zimdahl, Interacting dark energy and cosmological equations of state, Int. J. Mod. Phys. D **14**, 2319 (2005).
[135] B. Wang, Y. g. Gong, and E. Abdalla, Transition of the dark energy equation of state in an interacting holographic dark energy model, Phys. Lett. B **624**, 141 (2005).
[136] M. S. Berger and H. Shojaei, Interacting dark energy and the cosmic coincidence problem, Phys. Rev. D **73**, 083528 (2006).
[137] J. D. Barrow and T. Clifton, Cosmologies with energy exchange, Phys. Rev. D **73**, 103520 (2006).
[138] H. M. Sadjadi and M. Honardoost, Thermodynamics second law and omega $= -1$ crossing(s) in interacting holographic dark energy model, Phys. Lett. B **647**, 231 (2007).
[139] O. Bertolami, F. Gil Pedro, and M. Le Delliou, Dark energy-dark matter interaction and the violation of the equivalence principle from the Abell cluster A586, Phys. Lett. B **654**, 165 (2007).
[140] J. H. He and B. Wang, Effects of the interaction between dark energy and dark matter on cosmological parameters, J. Cosmol. Astropart. Phys. 06 (2008) 010.
[141] X. m. Chen, Y. g. Gong, and E. N. Saridakis, Phase-space analysis of interacting phantom cosmology, J. Cosmol. Astropart. Phys. 04 (2009) 001.
[142] S. Basilakos and M. Plionis, Is the interacting dark matter scenario an alternative to dark energy?, Astron. Astrophys. **507**, 47 (2009).
[143] M. B. Gavela, D. Hernandez, L. Lopez Honorez, O. Mena, and S. Rigolin, Dark coupling, J. Cosmol. Astropart. Phys. 07 (2009) 034.
[144] J. Väliviita, R. Maartens, and E. Majerotto, Observational constraints on an interacting dark energy model, Mon. Not. R. Astron. Soc. **402**, 2355 (2010).
[145] L. P. Chimento, Linear and nonlinear interactions in the dark sector, Phys. Rev. D **81**, 043525 (2010).
[146] M. Gavela, L. Lopez Honorez, O. Mena, and S. Rigolin, Dark coupling and gauge invariance, J. Cosmol. Astropart. Phys. 11 (2010) 044.

[147] T. Harko and F. S. N. Lobo, Irreversible thermodynamic description of interacting dark energy-dark matter cosmological models, Phys. Rev. D **87**, 044018 (2013).

[148] S. Pan and S. Chakraborty, Will there be again a transition from acceleration to deceleration in course of the dark energy evolution of the universe?, Eur. Phys. J. C **73**, 2575 (2013).

[149] Y. H. Li and X. Zhang, Large-scale stable interacting dark energy model: Cosmological perturbations and observational constraints, Phys. Rev. D **89**, 083009 (2014).

[150] W. Yang and L. Xu, Testing coupled dark energy with large scale structure observation, J. Cosmol. Astropart. Phys. 08 (2014) 034.

[151] W. Yang and L. Xu, Cosmological constraints on interacting dark energy with redshift-space distortion after Planck data, Phys. Rev. D **89**, 083517 (2014).

[152] R. C. Nunes and E. M. Barboza, Dark matter-dark energy interaction for a time-dependent EoS parameter, Gen. Relativ. Gravit. **46**, 1820 (2014).

[153] V. Faraoni, J. B. Dent, and E. N. Saridakis, Covariantizing the interaction between dark energy and dark matter, Phys. Rev. D **90**, 063510 (2014).

[154] V. Salvatelli, N. Said, M. Bruni, A. Melchiorri, and D. Wands, Indications of a Late-Time Interaction in the Dark Sector, Phys. Rev. Lett. **113**, 181301 (2014).

[155] W. Yang and L. Xu, Coupled dark energy with perturbed Hubble expansion rate, Phys. Rev. D **90**, 083532 (2014).

[156] S. Pan, S. Bhattacharya, and S. Chakraborty, An analytic model for interacting dark energy and its observational constraints, Mon. Not. R. Astron. Soc. **452**, 3038 (2015).

[157] J. L. Cui, L. Yin, L. F. Wang, Y. H. Li, and X. Zhang, A closer look at interacting dark energy with statefinder hierarchy and growth rate of structure, J. Cosmol. Astropart. Phys. 09 (2015) 024.

[158] Y. H. Li, J. F. Zhang, and X. Zhang, Testing models of vacuum energy interacting with cold dark matter, Phys. Rev. D **93**, 023002 (2016).

[159] R. C. Nunes, S. Pan, and E. N. Saridakis, New constraints on interacting dark energy from cosmic chronometers, Phys. Rev. D **94**, 023508 (2016).

[160] W. Yang, H. Li, Y. Wu, and J. Lu, Cosmological constraints on coupled dark energy, J. Cosmol. Astropart. Phys. 10 (2016) 007.

[161] S. Pan and G. S. Sharov, A model with interaction of dark components and recent observational data, Mon. Not. R. Astron. Soc. **472**, 4736 (2017).

[162] A. Mukherjee and N. Banerjee, In search of the dark matter dark energy interaction: A kinematic approach, Classical Quantum Gravity **34**, 035016 (2017).

[163] G. S. Sharov, S. Bhattacharya, S. Pan, R. C. Nunes, and S. Chakraborty, A new interacting two fluid model and its consequences, Mon. Not. R. Astron. Soc. **466**, 3497 (2017).

[164] M. Shahalam, S. D. Pathak, S. Li, R. Myrzakulov, and A. Wang, Dynamics of coupled phantom and tachyon fields, Eur. Phys. J. C **77**, 686 (2017).

[165] R. Y. Guo, Y. H. Li, J. F. Zhang, and X. Zhang, Weighing neutrinos in the scenario of vacuum energy interacting with cold dark matter: Application of the parameterized post-Friedmann approach, J. Cosmol. Astropart. Phys. 05 (2017) 040.

[166] R. G. Cai, N. Tamanini, and T. Yang, Reconstructing the dark sector interaction with LISA, J. Cosmol. Astropart. Phys. 05 (2017) 031.

[167] W. Yang, N. Banerjee, and S. Pan, Constraining a dark matter and dark energy interaction scenario with a dynamical equation of state, Phys. Rev. D **95**, 123527 (2017).

[168] W. Yang, S. Pan, and D. F. Mota, Novel approach toward the large-scale stable interacting dark-energy models and their astronomical bounds, Phys. Rev. D **96**, 123508 (2017).

[169] S. Pan, A. Mukherjee, and N. Banerjee, Astronomical bounds on a cosmological model allowing a general interaction in the dark sector, Mon. Not. R. Astron. Soc. **477**, 1189 (2018).

[170] W. Yang, S. Pan, R. Herrera, and S. Chakraborty, Large-scale (in) stability analysis of an exactly solved coupled dark-energy model, Phys. Rev. D **98**, 043517 (2018).

[171] W. Yang, S. Pan, L. Xu, and D. F. Mota, Effects of anisotropic stress in interacting dark matter-dark energy scenarios, Mon. Not. R. Astron. Soc. **482**, 1858 (2019).

[172] W. Yang, S. Pan, and A. Paliathanasis, Cosmological constraints on an exponential interaction in the dark sector, Mon. Not. R. Astron. Soc. **482**, 1007 (2019).

[173] R. von Marttens, L. Casarini, D. F. Mota, and W. Zimdahl, Cosmological constraints on parametrized interacting dark energy, Phys. Dark Universe **23**, 100248 (2019).

[174] W. Yang, N. Banerjee, A. Paliathanasis, and S. Pan, Reconstructing the dark matter and dark energy interaction scenarios from observations, Phys. Dark Universe **26**, 100383 (2019).

[175] A. Paliathanasis, S. Pan, and W. Yang, Dynamics of nonlinear interacting dark energy models, Int. J. Mod. Phys. D **28**, 1950161 (2019).

[176] J. D. Barrow and G. Kittou, Non-linear interactions in cosmologies with energy exchange, Eur. Phys. J. C **80**, 120 (2020).

[177] W. Yang, S. Pan, R. C. Nunes, and D. F. Mota, Dark calling dark: Interaction in the dark sector in presence of neutrino properties after Planck CMB final release, J. Cosmol. Astropart. Phys. 04 (2020) 008.

[178] C. van de Bruck and J. Morrice, Disformal couplings and the dark sector of the universe, J. Cosmol. Astropart. Phys. 04 (2015) 036.

[179] C. G. Böehmer, N. Tamanini, and M. Wright, Interacting quintessence from a variational approach Part I: Algebraic couplings, Phys. Rev. D **91**, 123002 (2015).

[180] C. G. Böehmer, N. Tamanini, and M. Wright, Interacting quintessence from a variational approach Part II: Derivative couplings, Phys. Rev. D **91**, 123003 (2015).

[181] J. Gleyzes, D. Langlois, M. Mancarella, and F. Vernizzi, Effective theory of interacting dark energy, J. Cosmol. Astropart. Phys. 08 (2015) 054.

[182] G. D'Amico, T. Hamill, and Nemanja Kaloper, Quantum field theory of interacting dark matter/dark energy: Dark monodromies, Phys. Rev. D **94**, 103526 (2016).

[183] S. Pan, G. S. Sharov, and W. Yang, Field theoretic interpretations of interacting dark energy scenarios and recent observations, Phys. Rev. D **101**, 103533 (2020).

[184] S. Basilakos, N. E. Mavromatos, and J. Solá Peracaula, Gravitational and Chiral anomalies in the running vacuum universe and matter-antimatter asymmetry, Phys. Rev. D **101**, 045001 (2020).
[185] S. Basilakos, N. E. Mavromatos, and J. Solá Peracaula, Quantum anomalies in string-inspired running vacuum universe: Inflation and axion dark matter, Phys. Lett. B **803**, 135342 (2020).
[186] Y. Wang, D. Wands, G. B. Zhao, and L. Xu, Post-*Planck* constraints on interacting vacuum energy, Phys. Rev. D **90**, 023502 (2014).
[187] W. Yang, S. Pan, E. Di Valentino, B. Wang, and A. Wang, Forecasting interacting vacuum-energy models using gravitational waves, J. Cosmol. Astropart. Phys. 05 (2020) 050.
[188] C. G. Park and B. Ratra, Using the tilted flat-ΛCDM and the untilted nonflat ΛCDM inflation models to measure cosmological parameters from a compilation of observational data, Astrophys. J. **882**, 158 (2019).
[189] F. Beutler, C. Blake, M. Colless, D. H. Jones, L. Staveley-Smith, L. Campbell, Q. Parker, W. Saunders, and F. Watson, The 6dF Galaxy survey: Baryon acoustic oscillations and the local Hubble constant, Mon. Not. R. Astron. Soc. **416**, 3017 (2011).
[190] A. J. Ross, L. Samushia, C. Howlett, W. J. Percival, A. Burden, and M. Manera, The clustering of the SDSS DR7 main Galaxy sample C I. A 4 per cent distance measure at $z = 0.15$, Mon. Not. R. Astron. Soc. **449**, 835 (2015).
[191] S. Alam *et al.* (BOSS Collaboration), The clustering of galaxies in the completed SDSS-III Baryon oscillation spectroscopic survey: Cosmological analysis of the DR12 galaxy sample, Mon. Not. R. Astron. Soc. **470**, 2617 (2017).
[192] E. Krause *et al.* (DES Collaboration), Dark energy survey year 1 results: Multi-probe methodology and simulated likelihood analyses, arXiv:1706.09359.
[193] A. Lewis and S. Bridle, Cosmological parameters from CMB and other data: A Monte Carlo approach, Phys. Rev. D **66**, 103511 (2002).
[194] A. Lewis, A. Challinor, and A. Lasenby, Efficient computation of CMB anisotropies in closed FRW models, Astrophys. J. **538**, 473 (2000).
[195] A. Gelman and D. Rubin, Inference from iterative simulation using multiple sequences, Stat. Sci. **7**, 457 (1992).
[196] M. Doran, C. M. Muller, G. Schafer, and C. Wetterich, Gauge-invariant initial conditions and early time perturbations in quintessence universes, Phys. Rev. D **68**, 063505 (2003).
[197] E. Majerotto, J. Väliviita, and R. Maartens, Adiabatic initial conditions for perturbations in interacting dark energy models, Mon. Not. R. Astron. Soc. **402**, 2344 (2010).